Regge-Pole Model for πp, pp, and $\bar{p}p$ Scattering*

WILLIAM RARITA†
Physics Department, University of California, Berkeley, California

AND

ROBERT J. RIDDELL, JR., AND CHARLES B. CHIU
Lawrence Radiation Laboratory, University of California, Berkeley, California

AND

ROGER J. N. PHILLIPS
Atomic Energy Research Establishment, Harwell, England

(Received 28 June 1967)

A model for high-energy πp, pp, and $\bar{p}p$ elastic scattering at small momentum transfer is presented, based on the assumed dominance of a few Regge poles in the crossed channel. For πp scattering these are the P, P', and ρ poles; for pp and $\bar{p}p$, ignoring isospin dependence, they are P, P', and ω. This model fits a wide variety of data, including the differential cross sections that shrink for pp but not for πp or $\bar{p}p$, recent results from Brookhaven on total cross sections and ratios of the real to imaginary parts of the forward scattering amplitude, and also recent πp and pp polarization results, but it gives zero polarization for πp charge-exchange scattering. (Although the latter disagrees with experiment, additions to the model to correct this insufficiency would affect the other results but little.) The factorization property of Regge poles is tested by these fits to data for the P and P' couplings.

I. INTRODUCTION

THE idea that high-energy scattering at small momentum transfer may be dominated by a few Regge poles in the crossed channel[1] has recently proved successful in fitting a variety of two-body scattering and reaction data.[2] The present paper extends previous work by showing that a wide range of πp, pp, and $\bar{p}p$ scattering data may be simultaneously fitted by a model using the P, P', ω, and ρ Regge poles.

The significance of simultaneous fitting to different processes is that, in addition to requiring that the same trajectories are important in various processes, the factorization constraints characteristic of Regge poles are tested. In the model reported here, factorization relates the ratios of spin flip to non-flip in the P and P' residue functions. Before high-energy polarization was measured, such relations were tested rather weakly[3]; and in "spinless" models they played no part at all.

In Secs. II and III we describe the formalism and parametrization of scattering amplitudes and the data used. Section IV gives the results found by adjusting the model parameters, and illustrates the fit to data. A discussion of the results is given in Sec. V, together with predictions of the model for $\pi\pi$ scattering, $\bar{p}p$ polarization, and second-rank polarization tensors for πp and pp scattering. Some of these predictions may soon be tested experimentally. Finally, five Appendices give supplementary discussions about: (A) the unitarity limit for an exponential diffraction peak, (B) partial-wave projections and unitarity tests, (C) polarization effects, (D) the way secondary Regge poles affect shrinking, and (E) the simplifications in notation and comprehension which can be obtained through the use of vector notation for the scattering amplitudes.

II. REGGE-POLE MODEL FOR πp, pp, AND $\bar{p}p$ SCATTERING

As has been found in earlier studies,[3,4] at least three Regge poles are needed to describe πp scattering: the two vacuum poles P and P', and the isovector pole ρ. We have restricted our analysis to these three, assuming them to dominate in the processes of interest. Following Singh[5] and subsequent analyses,[4] we introduce two amplitudes A' and B, and parametrize the Regge-pole contributions to them as follows[6]:

$$A'=C_0\exp(C_1t)\alpha(\alpha+1)\xi(E_L/E_0)^\alpha \quad \text{for } P \text{ and } P' \tag{1}$$
$$=C_0[(1+C_2)\exp(C_1t)-C_2](\alpha+1)\xi(E_L/E_0)^\alpha \quad \text{for } \rho,$$

* This work was supported in part by the U. S. Atomic Energy Commission.
† Visiting scientist.
[1] G. F. Chew and S. C. Frautschi, Phys. Rev. Letters **7**, 394 (1961); S. C. Frautschi, M. Gell-Mann, and F. Zachariasen, Phys. Rev. **126**, 2204 (1962); V. N. Gribov, Zh. Eksperim. i Teor. Fiz. **41**, 667 (1961) [English transl.: Soviet Phys.—JETP **14**, 478 (1962)].
[2] For a recent survey, see R. J. N. Phillips, in *Strong and Weak Interactions, Present Problems* (Academic Press Inc., New York, 1966), p. 268 ff; or L. VanHove, in *Proceedings of the Thirteenth Annual International Conference on High-Energy Physics, Berkeley, California, 1966* (University of California Press, Berkeley, Calif., 1967).
[3] R. J. N. Phillips and W. Rarita, Phys. Rev. **139**, B1336 (1965).
[4] C. B. Chiu, R. J. N. Phillips, and W. Rarita, Phys. Rev. **153**, 1485 (1967).
[5] V. Singh, Phys. Rev. **129**, 1889 (1963).
[6] The amplitude A' is given by Singh in Ref. 5, Eq. (6.4), as

$$A'=A+\frac{(E_L+t/4M_N)}{(1-t/4M_n^2)}B,$$

where A and B are the invariant amplitudes. Thus, unless B has a zero at $t=4M_N^2$, A' will have a pole there. Since we are far from this point in the present analysis, we parametrize A' as an analytic function in the region of interest. A similar consideration also applies to the parametrization of the nucleon amplitudes b_1, b_2 [see Eqs. (15)–(17)].

$$B=D_0 \exp(D_1 t)\alpha^2(\alpha+1)\xi(E_L/E_0)^{\alpha-1} \quad \text{for } P \text{ and } P'$$
$$=D_0 \exp(D_1 t)\alpha(\alpha+1)\xi(E_L/E_0)^{\alpha-1} \quad \text{for } \rho, \tag{2}$$

where

$$\xi(t)=-[\exp(-i\pi\alpha)\pm 1]/\sin\pi\alpha \tag{3}$$

and

$$\alpha(t)=\alpha(0)+t\alpha'. \tag{4}$$

Here, $\alpha(t)$ is the trajectory, t is the squared momentum transfer, and $\xi(t)$ is the signature factor (with signature $+$ for P and P', and $-$ for ρ). E_L is the total pion lab-system energy, and E_0 is a scale constant chosen to be 1 BeV. The P and P' coefficients contain factors $\alpha(\alpha+1)$ to kill a ghost state at $\alpha=0$ and to nullify the amplitude at $\alpha=-1$; similarly, the ρ coefficients contain factors $(\alpha+1)$ to remove a nonsense state at $\alpha=-1$. In addition, all the B terms contain a factor α; this is necessary in the case of ρ, but not strictly necessary in the P and P' cases.[4,7,8]

For definiteness, let us take C_0 and D_0 to be the coefficients occurring in $\pi^- p$ elastic scattering. Then for $\pi^+ p$ scattering, the P and P' terms stay the same while ρ changes sign; for charge exchange, the P and P' terms vanish and ρ is multiplied by $-\sqrt{2}$.

Although it will not be explored here, a different parametrization for the P' amplitudes has also been investigated following the so-called no-compensation mechanism.[8,9] At $\alpha_{P'}=0$, for this mechanism both A' and B have to vanish (see Sec. V. viii of the Discussion.) In this case the parametrization for the amplitudes is

$$A'=C_0 \exp(C_1 t)\alpha^2(\alpha+1)^2\xi(E_L/E_0)^{\alpha}, \tag{1'}$$

$$B=D_0 \exp(D_1 t)\alpha^2(\alpha+1)\xi(E_L/E_0)^{\alpha-1}. \tag{2'}$$

Corresponding changes are made in the nucleon-nucleon amplitudes.

In terms of A' and B, experimental quantities are given by

$$\sigma_T(s)=\mathrm{Im}A'(s,t=0)/p, \tag{5}$$

$$\frac{d\sigma}{dt}(s,t)=\frac{1}{\pi s}\left(\frac{M_N}{4k}\right)^2\left[\left(1-\frac{t}{4M_N^2}\right)|A'|^2 - \frac{t}{4M_N^2}\left(\frac{4M_N^2p^2+st}{4M_N^2-t}\right)|B|^2\right], \tag{6}$$

$$P(s,t)=-\frac{\sin\theta}{16\pi s^{1/2}}\frac{\mathrm{Im}(A'B^*)}{(d\sigma/dt)}. \tag{7}$$

Here, s is the invariant square of total energy, p is the pion lab momentum, k is the c.m. momentum, θ is the c.m. angle, and $P(s,t)$ is the polarization parameter defined relative to the normal $\mathbf{p}_i\times\mathbf{p}_f$, where $\mathbf{p}_i$ and $\mathbf{p}_f$ are initial and final pion momenta.

[7] S. C. Frautschi, Phys. Rev. Letters **17**, 722 (1966).
[8] L. L. Wang, Phys. Rev. **153**, 1664 (1967).
[9] C. B. Chiu, S. Y. Chu, and L. L. Wang, Phys. Rev. **161**, 1563 (1967).

For pp and $\bar{p}p$ scattering, we assume that the P, P', and ω Regge poles dominate. Any small contribution from the ϕ is effectively absorbed in ω. The contributions of the ρ and A_2 to the total cross section have been found to be small by Phillips and Rarita.[10] Their part in the differential cross section (DCS) and the polarization can be estimated using the results of a recent analysis by Arbab and Dash[11] for np and $\bar{p}p$ charge-exchange scattering. For the DCS the contributions are of the order of 1%. The same model for the ρ gives to the polarization (in which the amplitude enters principally via an interference with the P, P', and ω) a contribution of a few percent, which, although not negligible, is about as large as the errors in the experimental measurements. Thus we feel that it is reasonable to ignore the ρ and A_2. Furthermore, since we confine ourselves to pp and $\bar{p}p$ elastic scattering, any ρ and A_2 pole contributions will behave similarly to ω and P', respectively, and may be supposed to be absorbed in the latter at least approximately.

Our pp and $\bar{p}p$ formalism follows that of Sharp and Wagner.[12] The five helicity amplitudes $\phi_1\cdots\phi_5$ have the following forms, for each of the above Regge poles:

$$\phi_1=\phi_3=\frac{M_N E_0\xi}{4\pi s^{1/2}}\left(\frac{E_L}{E_0}\right)^{\alpha}\eta_N^2, \tag{8}$$

$$\phi_2=-\phi_4=-\frac{M_N E_0\xi}{4\pi s^{1/2}}\left(\frac{E_L}{E_0}\right)^{\alpha}\phi_N^2, \tag{9}$$

$$\phi_5=-\frac{M_N E_0\xi}{4\pi s^{1/2}}\left(\frac{E_L}{E_0}\right)^{\alpha}\eta_N\phi_N, \tag{10}$$

where s, ξ, α, and E_0 have the same meanings as before, and E_L is now the total proton lab-system energy. The factor functions η_N and ϕ_N embody the factorization property of Regge-pole couplings in the nucleon-nucleon system. The signs given above are appropriate to $\bar{p}p$ amplitudes; for pp amplitudes, the ω terms have opposite signs.

The factor functions η_N and ϕ_N are related to Gell-Mann's[13] η_1 and η_2 by[14]

$$\eta_N=\eta_1, \tag{11}$$

$$\phi_N=(-t/4M_N^2)^{1/2}(\eta_1-\eta_2). \tag{12}$$

[10] R. J. N. Phillips and W. Rarita, Phys. Rev. Letters **14**, 502 (1965).
[11] F. Arbab and J. Dash, Phys. Rev. **163**, 1603 (1967).
[12] D. H. Sharp and W. G. Wagner, Phys. Rev. **131**, 2226 (1963); W. G. Wagner, Phys. Rev. Letters **10**, 202 (1963).
[13] M. Gell-Mann, in *Proceedings of the 1962 Annual International Conference on High-Energy Nuclear Physics, at CERN*, edited by J. Prentki (CERN, Geneva, 1962), p. 533.
[14] In Ref. 12, the ϕ_N relation to η_1 and η_2 as given by Wagner has a sign error which has led to some confusion. In R. J. N. Phillips and W. Rarita, University of California Radiation Laboratory Report No. UCRL-16185, 1965 (unpublished), for example, the ϕ_N that is used is the negative of the ϕ_N we use here. We are grateful to W. G. Wagner for confirming this statement, and to J. V. Lepore and one of us (R.J.R.) for providing an independent check.

It is convenient for parametrization to express η_N and ϕ_N in terms of two functions b_1 and b_2, as follows[12]:

$$\eta_N = b_1 - (\alpha t/4M_N^2)b_2\,, \tag{13}$$

$$\phi_N = (-t/4M_N^2)^{1/2}(b_1 - \alpha b_2)\,. \tag{14}$$

This last step allows a convenient connection to be made between the pp and the πp parameters, because factorization gives[3,14]

$$\frac{A'}{E_L B} = \frac{\eta_1 + \eta_2 t/(4M_N^2 - t)}{\eta_2} = \frac{b_1}{\alpha b_2(1 - t/4M_N^2)}\,, \tag{15}$$

where E_L is the energy of the pion in the laboratory system. Hence, for the P and P' Regge poles it is enough to parametrize b_1; b_2 is then determined by b_1 and the πp parametrization.

The functions b_1 and b_2 are parametrized as follows:

$$\begin{aligned} b_1 &= F_0 \exp(F_1 t)[\alpha(\alpha+1)]^{1/2} \quad \text{for } P \text{ and } P' \\ &= F_0 \exp(F_1 t)[(1 - t/t_0)(\alpha+1)]^{1/2} \quad \text{for } \omega\,, \end{aligned} \tag{16}$$

$$b_2 = G_0 \exp(G_1 t)[(1 - t/t_0)(\alpha+1)]^{1/2}(1 - t/4M_N^2)^{-1} \quad \text{for } \omega\,, \tag{17}$$

where F_0, F_1, G_0, G_1, and t_0 are adjustable parameters. The factors $\alpha^{1/2}$ and $(\alpha+1)^{1/2}$ are present to remove ghost or nonsense states at $\alpha = 0$ and -1. The extra factor $(1-t/t_0)^{1/2}$ in the ω-factor functions is introduced to produce a sign change in all the ω residues at $t = t_0$, as is required to explain the crossover of pp and $\bar{p}p$ differential cross sections.[15]

From the forms assumed for A', B, and b_1, we then find for the P, P' poles

$$b_2 = G_0 \exp(G_1 t)[\alpha(\alpha+1)]^{1/2}(1 - t/4M_N^2)^{-1}\,,$$

where $G_0 = F_0(D_0/C_0)$ and $G_1 = F_1 + (D_1 - C_1)$.

An alternative parametrization of the ω residues has also been tried. In this the sign change in b_1^2 and b_2^2 is achieved by having α_ω pass through zero while the couplings "choose nonsense"—the original Gell-Mann ghost-killing mechanism.[13] This makes the sign change physically understandable, by linking it with the point $\alpha_\omega = 0$. In this case [note that these forms differ from those of Ref. 9 in their $(\alpha+1)$ factors for this mechanism],

$$b_{1\omega} = F_0 \exp(F_1 t)[\alpha(\alpha+1)]^{1/2}\,, \tag{16$'$}$$

$$b_{2\omega} = G_0 \exp(G_1 t)[(\alpha+1)/\alpha]^{1/2}(1 - t/4M_N^2)^{-1}\,. \tag{17$'$}$$

With this type of solution we used a curved ω trajectory;

$$\alpha(t) = \alpha_0 + \alpha_1 t + \alpha_2 t^2\,. \tag{4$'$}$$

Experimental pp and $\bar{p}p$ quantities are given in terms of the helicity amplitudes as follows:

$$\sigma_T(s) = \frac{2\pi}{k}\,\mathrm{Im}(\phi_1 + \phi_3)_{t=0}\,, \tag{18}$$

$$\frac{d\sigma}{dt}(s,t) = \frac{\pi}{2k^2}(|\phi_1|^2 + |\phi_2|^2 + |\phi_3|^2 + |\phi_4|^2 + 4|\phi_5|^2)\,, \tag{19}$$

$$P(s,t) = \frac{\pi}{2k^2}\,\frac{\mathrm{Im}[\phi_5(\phi_1 + \phi_2 + \phi_3 - \phi_4)^*]}{(d\sigma/dt)}\,, \tag{20}$$

with our previous notation and conventions for $P(s,t)$ and k as stated following Eq. (7). Compact expressions in terms of the factor functions η_N and ϕ_N can be derived.[12]

Appendix C contains a discussion of second-rank polarization tensors, for πp, pp, and $\bar{p}p$ scattering, with formulas for the experimental quantities.

For $\pi\pi$ scattering, factorization allows us to predict the P and P' couplings. Let $A_{\pi\pi}(s,t)$ be the scattering amplitude, so normalized that

$$\sigma_T(s) = \mathrm{Im}A(s, t=0)/s\,, \tag{21}$$

and then

$$\frac{d\sigma}{dt}(s,t) = \frac{1}{16\pi s^2}|A|^2\,. \tag{22}$$

Then asymptotically $A_{\pi\pi}$ has the form[16]

$$A_{\pi\pi}(s,t) = \xi s_0(s/s_0)^\alpha \eta_\pi^2\,, \tag{23}$$

where $\xi(t)$ is the signature factor as before, and the scale constant is $s_0 = 2M_N E_0$. The pion-factor function occurs also in the πp amplitudes; for example, $A_{\pi N}'$ has the asymptotic form[12,13]

$$\begin{aligned} A_{\pi N}' &= \xi E_0(s/s_0)^\alpha b_1 \eta_\pi \\ &= \xi\left(\frac{s_0}{2M_N}\right)\left(\frac{s}{s_0}\right)^\alpha \frac{[\eta_N + (-t/4M_N^2)^{1/2}\phi_N]}{(1 - t/4M_N^2)}\eta_\pi\,. \end{aligned} \tag{24}$$

(Although $A_{\pi N}'$ appears to have a pole at $t = 4M_N^2$, the parametrization which we use actually produces a compensating zero in the numerator.) Hence, using Eqs. (8)-(10), we can express the P and P' terms at given s and t in terms of the πN and NN contributions:

$$A_{\pi\pi} = \frac{M_N^2}{2\pi s^{1/2}}\left(1 - \frac{t}{4M_N^2}\right)^2 \times \frac{[A_{\pi N}']^2}{[\phi_1 + (t/4M_N^2)\phi_2 - 2(-t/4M_N^2)^{1/2}\phi_5]}\,. \tag{25}$$

For our parametrization we find

$$\eta_\pi = (C_0/E_0 F_0)\exp[(C_1 - F_1)t][\alpha(\alpha+1)]^{1/2}\,. \tag{26}$$

One may ask why we did not use the Sharp-Wagner formalism for πp scattering also, simply parametrizing η_π, η_N, and ϕ_N directly? The reason is that this formalism rests on extreme asymptotic approximations;

[15] W. Rarita and V. L. Teplitz, Phys. Rev. Letters **12**, 206 (1964).

[16] The P and P' contributions considered here are independent of isospin. The amplitudes for $I = 0$, 1, and 2 are equal; the result given is for the sum of the three channels.

all corrections of order $1/s$ are ignored—including the difference between $\sin\theta$ and 1. For πp scattering at $t=-1(\text{BeV}/c)^2$ and $E_L=6$ BeV, $\sin\theta\approx0.6$ (though at $E_L=18$ BeV the value drops to $\sin\theta\approx0.3$). The πp analysis seems to warrant a more careful treatment, and we therefore use the A' and B amplitudes. The NN analysis, on the other hand, has additional approximations anyway, so the Sharp-Wagner approximations are more acceptable here.

III. DATA SELECTION

For πN scattering we use the following data which have incident momenta from 5.9 BeV/c upward, and squared momentum transfer $|t|<1$ $(\text{BeV}/c)^2$:

Total π^+p and π^-p cross sections; 16 data points.[17]
Elastic π^+p and π^-p differential cross sections; altogether 45 data points.[18]

Charge-exchange $\pi^-+p\rightarrow\pi^0+n$ cross sections; 56 data points.[19]

Elastic π^+p and π^-p polarizations; 85 data points.[20]
The phase of the forward π^+p and π^-p amplitudes, from Coulomb interference measurements; 9 data points.[21]

We do not use the recent charge-exchange polarization data.[22] In our model, such polarization is always zero, and it would have to be explained as interference with some background effect.

For pp and $\bar{p}p$ scattering, the data used are the following:

Total pp and $\bar{p}p$ cross sections; 24 data points.[17]
Elastic pp and $\bar{p}p$ differential cross sections; 161 data points.[23]

Elastic pp polarization; 43 data points.[24]

Coulomb interference measurements of the phase of the forward pp amplitude; 12 data points.[25]

Recently new data on total cross sections and the ratio of the real to the imaginary part of the forward scattering amplitude have become available.[26] These data have been used as an alternative to some of the preceding data, including:

Total π^+p and π^-p cross sections; 28 data points.

Phase of the forward π^+p and π^-p amplitudes; 21 data points.

Total pp cross sections; 18 data points.

Phase of the forward pp amplitudes; 7 data points.

In addition to these new measurements of previously measured quantities, the phase of the forward $\bar{p}p$ amplitudes has now been measured at one energy.

Lindenbaum[26] has given two sets of results for the phase of the forward scattering amplitude for $\pi^\pm p$, according to two theoretical analyses of the Coulomb corrections, and we have compared our fits with each.

None of the above NN or $\bar{N}N$ data themselves imply any isospin dependence, and we have not tried to fit such a dependence explicitly. Thus we do not use any data for pn or $\bar{p}n$ scattering, nor for np or $\bar{p}p$ charge exchange, though some is available.[17,27] Our reasons are these:

(a) There are many Regge poles that could bring isospin dependence to NN and $\bar{N}N$ scattering (e.g., ρ, A_2, π, B, A_1), compared to ρ alone for πN, so we can scarcely hope for a unique prescription.

(b) Even with all these poles, there are still some difficulties in understanding the charge-exchange data.[2] This is a special question that should be treated separately.

[17] W. Galbraith, E. W. Jenkins, T. F. Kycia, B. A. Leontic, R. H. Phillips, A. L. Read, and R. Rubinstein, Phys. Rev. **138**, B913 (1965).

[18] K. J. Foley, S. J. Lindenbaum, W. A. Love, S. Ozaki, J. J. Russell, and L. C. L. Yuan, Phys. Rev. Letters **11**, 425 (1963); D. Harting, P. Blackall, B. Elsner, A. C. Helmholz, W. C. Middelkoop, B. Powell, B. Zacharov, P. Zanella, P. Dalpiaz, M. N. Focacci, S. Focardi, G. Giacomelli, L. Monari, J. A. Beaney, R. A. Donald, P. Mason, L. W. Jones, and D. O. Caldwell, Nuovo Cimento **38**, 60 (1965).

[19] A. V. Stirling, P. Sonderegger, J. Kirz, P. Falk-Vairant, O. Guisan, C. Bruneton, P. Borgeaud, M. Yvert, J. P. Guilland, C. Caverzasio, and B. Amblard, Phys. Rev. Letters **14**, 763 (1965); I. Mannelli, A. Bigi, R. Carrara, M. Wahlig, and L. Sodickson, *ibid.* **14**, 408 (1965).

[20] M. Borghini, G. Coignet, L. Dick, L. di Lella, A. Michaelowicz, P. C. Macq, and J. C. Olivier, Phys. Letters **21**, 114 (1966); and Dr. Dick and Dr. di Lella (private communication).

[21] K. J. Foley, R. S. Gilmore, R. S. Jones, S. J. Lindenbaum, W. A. Love, S. Ozaki, E. H. Willen, R. Yamada, and L. C. L. Yuan, Phys. Rev. Letters **14**, 862 (1965).

[22] P. Bonamy, P. Borgeaud, S. Brehin, C. Bruneton, P. Falk-Vairant, O. Guisan, P. Sonderegger, C. Caverzasio, J. P. Guilland, J. Schneider, M. Yvert, I. Mannelli, F. Sergiampietri, and M. L. Vincelli, Phys. Letters **23**, 501 (1966).

[23] K. J. Foley, S. J. Lindenbaum, W. A. Love, S. Ozaki, J. J. Russell, and L. C. L. Yuan, Phys. Rev. Letters **10**, 376 (1963); **11**, 425, 503 (1963); **15**, 45 (1965).

[24] M. Borghini, G. Coignet, L. Dick, K. Kuroda, L. di Lella, A. Michaelowicz, P. C. Macq, and J. C. Olivier, Phys. Letters **24B**, 77 (1967).

[25] E. Lohrmann, H. Meyer, and H. Winzeler, Phys. Letters **13**, 78 (1964); L. Kirillova, L. Khristov, V. Nikitin, M. Shafranova, L. Stanov, L. Sviridov, Z. Korbel, L. Rob, P. P. Markov, Kh. Tchernev, T. Todorov, and M. Zlateva, *ibid.* **13**, 93 (1964); G. Belletini, G. Cocconi, A. N. Diddens, E. Lillethun, J. Pahl, J. P. Scanlon, J. Walters, A. M. Wetherell, and P. Zanella, *ibid.* **14**, 164 (1965); **19**, 341 (1965); A. E. Taylor, I. L. Watkins, A. Ashmore, W. S. Chapman, D. F. Falla, W. H. Range, D. B. Scott, A. Astbury, F. Capocci, J. F. Crawford, M. Sproul, and T. G. Walker, *ibid.* **14**, 54 (1965); K. J. Foley, R. S. Gilmore, R. S. Jones, S. J. Lindenbaum, W. A. Love, S. Ozaki, E. M. Willen, R. Yamada, and L. C. L. Yuan, Phys. Rev. Letters **14**, 74 (1965); L. Kirillova, V. Nikitin, V. Pantuev, V. Sviridov, L. Strunov, M. Khachaturyan, L. Khristov, M. Shafronava, Z. Korbel, L. Rob, S. Damyanov, A. Zlateva, Z. Zlatanov, V. Jordanov, Kh. Kanazirsky, P. Markov, T. Todorov, Kh. Chernev, N. Dalkhazhav, and D. Tuvdendorzh, Yadern. Fiz. **1**, 533 (1965) [English transl.: Soviet J. Nucl. Phys. **1**, 379 (1965)]; G. Bellettini, G. Cocconi, A. N. Diddens, E. Lillethun, J. P. Scanlon, and A. M. Wetherell, Phys. Letters **19**, 705 (1965).

[26] S. J. Lindenbaum, in *Proceedings of the Third Coral Gables Conference on Symmetry Principles at High Energy*, edited by B. Kursunoglu, A. Perlmutter, and I. Sakmar (W. H. Freeman and Co., San Francisco, 1966).

[27] G. Manning, A. G. Parham, J. D. Jafar, H. B. van der Raay, D. H. Reading, D. G. Ryan, B. D. Jones, J. Malos, and N. H. Lipman, Nuovo Cimento **41**, 167 (1966); P. Astbury, G. Brantti, G. Finocchiaro, A. Michelini, D. Websdale, C. H. West, E. Polgar, W. Beusch, W. E. Fischer, B. Gobbi, and M. Pepin, Phys. Letters **23**, 160 (1966); M. N. Kreisler, F. Martin, M. L. Perl, M. J. Longo, and S. T. Powell, Phys. Rev. Letters **16**, 1217 (1966).

TABLE I. P Regge-pole parameters.

Solution	$\alpha(0)$	$\alpha'(\mathrm{BeV}^{-2})$	C_0(mb BeV)	$C_1(\mathrm{BeV}^{-2})$	$D_0/C_0(\mathrm{BeV}^{-1})$	$D_1-C_1(\mathrm{BeV}^{-2})$	$F_0(\mathrm{mb}^{1/2})$	$F_1(\mathrm{BeV}^{-2})$
1	1.0	0.12	7.23	2.36	−3.69	7.02	3.80	2.09
1a	1.0	0.11	7.09	2.38	−3.59	8.05	3.88	2.17
2	1.0	0.00	...	...	−4.36	−0.35	3.29	3.25
3	1.0	0.29	10.24	2.18	−3.11	10.32	4.17	1.77

TABLE II. P' Regge-pole parameters.

Solution	$\alpha(0)$	$\alpha'(\mathrm{BeV}^{-2})$	C_0(mb BeV)	$C_1(\mathrm{BeV}^{-2})$	$D_0/C_0(\mathrm{BeV}^{-1})$	$D_1-C_1(\mathrm{BeV}^{-2})$	$F_0(\mathrm{mb}^{1/2})$	$F_1(\mathrm{BeV}^{-2})$
1	0.73	1.50	16.35	0.44	−3.52	3.42	5.04	1.06
1a	0.73	1.50	16.91	0.24	−4.24	5.47	4.87	0.87
2	0.75	1.50	....	....	−5.61	−0.56	5.82	2.80
3	0.57	2.17	16.58	−2.99	−7.33	8.29	5.86	−0.93

(c) Isospin dependence is in fact small, giving corrections to total cross sections that are $\lesssim 5\%$, and charge exchange that is $\lesssim 1\%$ of elastic scattering, at energies of present interest.

(d) Although they are not explicitly included, at least some of the leading isospin terms from ρ and A_2 may be considered as implicitly included in the ω and P' terms, since they behave in the same way for pp and $\bar{p}p$ scattering. [See also the remarks on these poles in Sec. II following Eq. (7).]

Within the classes of data that are used, some selection is needed. There are too many available data points for the search program to handle efficiently, so in several cases we have taken representative subsets. For example, for π^-p charge exchange we took only the values of Stirling *et al.* of Ref. 19, after confirming that the data of Mannelli *et al.* agree with the former quite well. In our fitting of the data to the phenomenological forms assumed in Sec. II, we adjust the parameters to obtain values of χ^2 which are reasonable for the various classes of data. Thus the number of points retained for each type of data does not significantly affect the final result. Another problem is that certain data points, from different sources, strongly disagree. In such cases, we have sometimes eliminated these points, or have arbitrarily increased their quoted errors.

Note that for subsequent use the term "phase of the forward scattering amplitude" refers to the ratio of the real part to the imaginary part of the amplitude.

IV. RESULTS

We adjusted the model parameters to fit the data, using the CDC 6600 computer at Berkeley with programs based on a variable metric minimization method (VARMIT).[28] In this method a minimum for a function of many variables is obtained. For our use the function selected was the sum of the χ^2 for each point multiplied by a specific weight factor chosen for each type of data. These weight factors were varied until the χ^2 associated with each class of data had a reasonable value (see Table V).

Solutions (1) and (1a) are parametrized according to Eqs. (1)–(4) and (15)–(17). The difference between them comes from ρ-meson constraints which are only imposed to obtain solution (1a). (See Secs. V. v and V. xii.) The fit to the 211 πN data points and 240 NN data points gives the χ^2 values of 301 and 317, respectively, for solution (1). The parameters are presented in Tables I–IV, and in Table V we present the χ^2 value for each type of data for both solutions. The fit to the data and predictions for various energies up to 200 BeV are illustrated for solution (1) in Figs. 1–20. The results for solution (1a) are very similar to these fits.

Solution (2) is also parametrized in the same way as is solution (1), except that the ω amplitudes are parametrized according to Gell-Mann's ghost-killing mechanism given by Eqs. (16′) and (17′). In this case, we are able to obtain a satisfactory fit only to the NN data alone. As expected, this fit is much less restricted than is the fit to the combined data. With 240 NN data points, the obtained χ^2 value is 266, which is better than the corresponding value for solution (1), and is

TABLE III. ρ Regge-pole parameters.

Solution	$\alpha(0)$	$\alpha'(\mathrm{BeV}^{-2})$	C_0(mb BeV)	$C_1(\mathrm{BeV}^{-2})$	C_2	D_0(mb)	$D_1(\mathrm{BeV}^{-2})$
1	0.58	0.94	1.47	0.20	15.2	26.3	0.34
1a	0.58	1.01	1.51	2.39	1.48	29.4	0.14
2	...	...	...	...	...	...	...
3	0.57	0.99	1.57	2.02	1.65	29.1	0.11

[28] W. C. Davidson, Argonne National Laboratory Report No. ANL-5990, 1959 (unpublished). VARMIT is a version of this method developed by E. Beals at Lawrence Radiation Laboratory.

TABLE IV. ω Regge-pole parameters.

Solution	α_0	α_1(BeV^{-2})	α_2(BeV^{-4})	t_0(BeV^2)	F_0(mb$^{1/2}$)	F_1(BeV^{-2})	G_0/F_0	G_1-F_2(BeV^{-2})
1	0.45	0.31	...	−0.13	3.94	1.85	−16.4	4.47
1a	0.47	0.38	...	−0.13	3.82	1.70	−14.1	4.30
2	0.21	1.66	1.35	...	13.1	1.10	− 3.10	−0.08
3	0.36	0.32	...	−0.13	4.51	1.93	−13.1	3.56

only slightly poorer than the solution corresponding to the latter when only pp and $\bar{p}p$ data are used, for which $\chi^2=255$. A search for the fits for the combined πN and NN data gives a χ^2 of about 800; the corresponding value for solution (1) is 618. We present in Tables I–V for solution (2), the parameters for the NN amplitudes only, and the χ^2 values for individual groups of data.

The alternative data from Brookhaven[26] have also been fitted to give solution (3), using essentially the same parametrization as for solution (1). In this solution $\alpha_{P'}'$ tended to become quite large, so that the amplitudes for some data points came near to a pole in $\xi(t)$ at $\alpha=-2$. This pole was removed by multiplying the P and P' amplitudes by a factor $[\alpha(t)+2]/[\alpha(0)+2]$. In these data, several features stand out, aside from the significantly improved errors: First, the asymptotic limits to the πp and pp total cross sections are somewhat higher; secondly, the magnitude of the phase of the pp forward amplitudes is found to decrease with energy whereas previous data do not clearly indicate this trend. For asymptotically large energies, the Regge-pole model predicts a decreasing magnitude for the phase. Further, the magnitude of the π^+p phase is now found to be larger than the π^-p phase, whereas the reverse situation was formerly obtained. This new result is in agreement with the Regge-pole prediction (and the forward dispersion relation), whereas previous data were incompatible with it, although the stated error limits were large. The detailed parameters and the χ^2 for the individual groups of data found in this solution are presented in Tables I–V. The values of χ^2 for the magnitude of the phase of the $\pi^{\pm}p$ forward scattering

TABLE V. χ^2 fits to data.

Type	Number of points	Solution (1)	Solution (1a)	Solution (2)	Solution (3)
πN data:					
$\sigma_T(\pi^{\pm}p)$	16	9	11	...	...
	28	...	...	...	23
$\frac{\text{Re}A'(0)}{\text{Im}A'(0)}(\pi^{\pm}p)$	9	16	16	...	...
	21	...	...	...	10
$\frac{d\sigma}{dt}(\pi^{\pm}p)$	45	46	43	...	50
$\frac{d\sigma}{dt}(\pi^-p\to\pi^0n)$	56	90	90	...	94
$P(\pi^{\pm}p)$	85	140	141	...	137
NN data:					
$\sigma_T(pp)$	14	5	6	2	...
	18	...	...	...	11
$\sigma_T(\bar{p}p)$	10	16	15	9	17
$\frac{\text{Re}\phi_1(0)}{\text{Im}\phi_1(0)}(pp)$	12	28	28	24	...
	7	...	...	...	19
$\frac{\text{Re}\phi_1(0)}{\text{Im}\phi_1(0)}(\bar{p}p)$	1	...	...	...	4
$\frac{d\sigma}{dt}(pp,\bar{p}p)$	161	192	189	171	184
$P(pp)$	43	76	88	60	80
Total $\chi^2=$		618	627	266	629

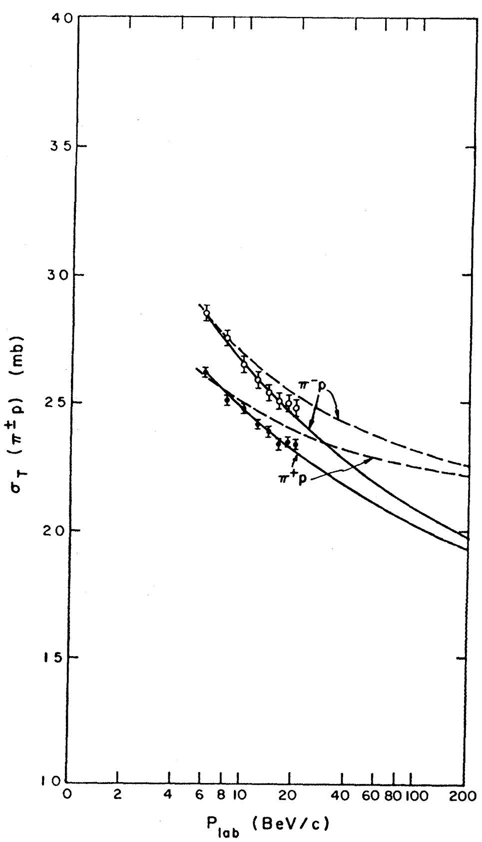

FIG. 1. Total cross sections for $\pi^{\pm}p$ from Ref. 17 compared with solution (1) with predictions up to 200 BeV/c (solid line) and also compared to solution (3) (dashed line).

amplitude data is only given for the Solov'ev correction. The data using the Bethe correction which are given in Fig. 22 have comparable error bars to the Solov'ev points. Aside from the $t=0$ fits to the data, the results are similar to those of solution (1), and with comparable χ^2. The fits to the $\pi^{\pm}p$ and pp total cross sections and to the phase of the $\pi^{\pm}p$ and pp forward scattering amplitudes are illustrated in Figs. 21–24. The ratio of the real to the imaginary part of the forward scattering amplitude for $\bar{p}p$ scattering at 12 BeV/c for solution (3) is found to be -0.096 as compared to an experimental value of $+0.02\pm0.032$ with an additional systematic error estimated as ±0.05. (This experimental value was obtained using the Bethe correction; this choice was also made for the pp data.) In Figs. 1, 2, 12, and 13 we have superimposed the result for fitting the Brookhaven data to show the change made by use of these data. As is seen, the asymptotic behavior of the total cross sections is markedly changed. (See Discussion, Sec. V. vii also).

Results using the no-compensation mechanism, Eqs. (1′) and (2′), are not reported here, and the reader is referred to Refs. 8, 9 for further information. This mechanism is also further discussed in Sec. V. viii.

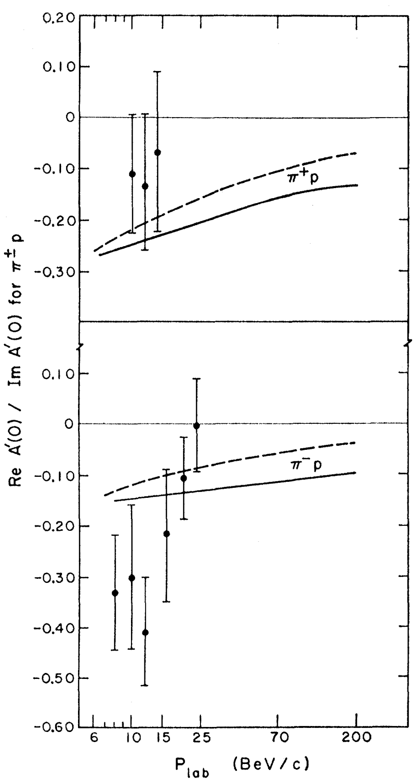

FIG. 2. The ratio of the real to the imaginary part of the forward scattering from Ref. 21 compared to solution (1) with predictions up to 200 BeV/c (solid line) and compared to solution (3) (dashed line).

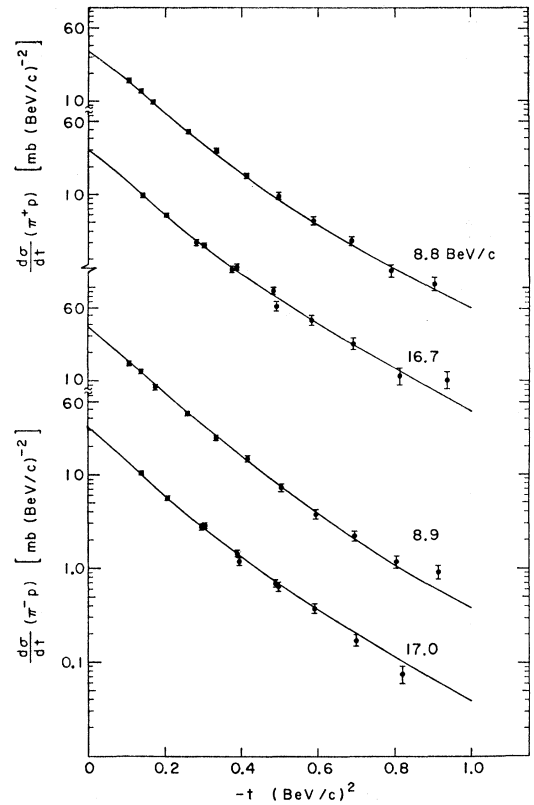

FIG. 3. π^+p differential cross sections at 8.8 and 16.7 BeV/c; and π^-p differential cross sections at 8.9 and 17.0 BeV/c compared to solution (1). Successive sets of data are spaced by a decade.

V. DISCUSSION

It is convenient to subdivide the discussion under separate headings.

(i) *Previous πN analyses.* The immediate predecessor to the present work is Ref. 4, which presented two solutions: (a) with small slopes for the P and P' trajectories, corresponding to earlier work generally[3]; and (b) with a big P' slope, in order to associate the dip and second maximum in the elastic $\pi^{\pm}p$ differential cross sections with a zero of $\alpha_{P'}$.

We have found reasonable over-all fits to both πN and NN data with solutions of type (b) only. Type (a) has not survived.

As to the $\pi^{\pm}p$ crossover effect, our solutions rely strongly on a sign change in A_ρ' (using $C_2\neq0$) as discussed in Ref. 3.

(ii) *Previous NN analyses.* Most of the earlier work[15,29,30] has not included spin dependence. Some work including the Berkeley polarization data[31] which

[29] F. Hadjioannu, R. J. N. Phillips, and W. Rarita, Phys. Rev. Letters 9, 183 (1962).
[30] T. O. Binford and B. R. Desai, Phys. Rev. 138, B1167 (1965).
[31] P. Grannis, J. Arens, F. Betz, O. Chamberlain, B. Dieterle, C. Schultz, G. Shapiro, H. Steiner, L. Van Rossum, and D. Weldon, Phys. Rev. 148, 1297 (1966).

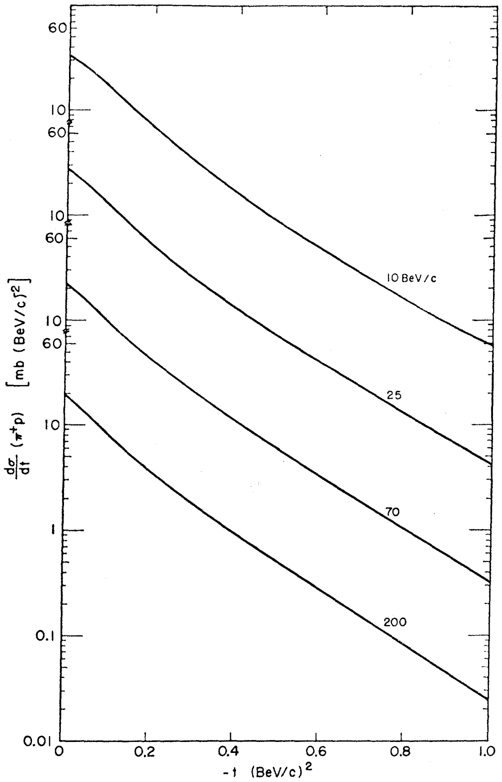

FIG. 4. π^+p differential cross sections predicted by solution (1) up to 200 BeV/c. Successive sets are spaced by a decade.

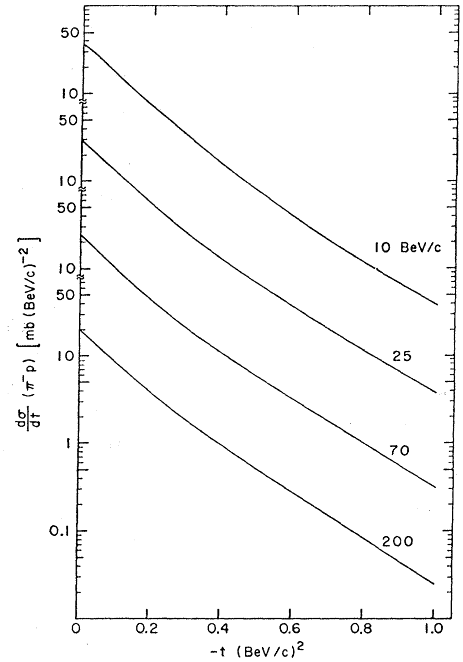

FIG. 5. π^-p differential cross sections predicted by solution (1) up to 200 BeV/c. Successive sets are spaced by a decade.

gave good fits has been reported[32,33] (See also the report referred to in Ref. 14.) The Berkeley data are not consistent with the more recent and more accurate CERN data of Borghini *et al.*,[24] and so we confine ourselves in this report to the latter.

(iii) *pp and $\bar{p}p$ crossover.* The fact that $d\sigma/dt$ curves for pp and $\bar{p}p$ cross at small $|t|$ is attributed to a sign change in an ω residue function.[15,30] In order that real analyticity of the residues and factorization be maintained, *all* ω residues have to vanish at the same point.

Hitherto, this vanishing has been regarded as a dynamical accident, and has simply been parametrized into the residue functions η_N^2, ϕ_N^2, and $\eta_N\phi_N$. Solutions (1) and (3) embody this view. It is conceivable, however, that this vanishing is associated with $\alpha_\omega(t)$ going through zero, while the couplings "choose nonsense" (see Sec. II). This idea is attractive since it relates the vanishing point of α_ω to the rest of the dynamics. Solution (2), with the alternative parametrization of Eqs. (16′)–(17′) and (4′), embodies this idea. Although the fit to the NN data is a respectable one, the fit to the combined πN and NN data is rather poor. Nevertheless, we believe that an explanation along these lines is not completely excluded. The ω trajectory obtained here and its relation to the physical ω meson is illustrated in Fig. 25. For comparison, in the same figure we also present the ω and ρ trajectories for solution (1).

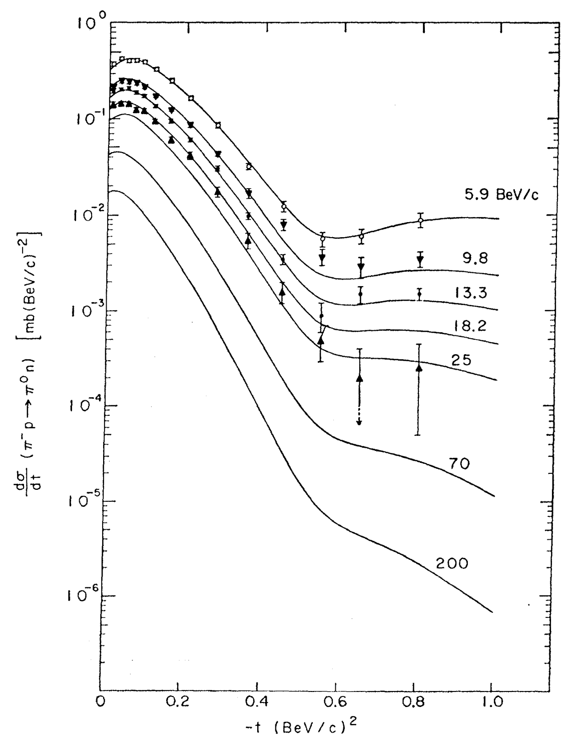

FIG. 6. $\pi^-+p\rightarrow\pi^0+n$ differential cross sections at 5.9, 9.8, 13.3, and 18.2 BeV/c compared to solution (1), with predictions up to 200 BeV/c.

[32] V. Flores-Maldonado, Phys. Rev. **155**, 1773 (1967).

[33] W. Rarita, in 200-BeV Accelerator: Study on Experimental Use, Vol. 3, 1966 Summer Study, Lawrence Radiation Laboratory Report No. UCRL-16830 (unpublished).

We note that extrapolation of the ρ trajectory to positive t leads to a mass of 670 MeV, in reasonable agreement with the experimental value. On the other hand, the ω trajectory in this case has a small slope and and a significant curvature is needed for $t>0$ for the ω trajectory to pass through the physical value. (For further discussion on the small slope of the ω, see Sec. V.ix.) This should not be surprising since the composite ω used is undoubtedly modified by effects of the ϕ, ρ, and low-lying trajectories which are lumped together in our model. The trajectory for solution (2) actually turns over near $t=-0.6$ $(\mathrm{BeV}/c)^2$. This peculiar situation is associated with the particular polynomial function that we have used. We expect that the fit beyond $t=-0.6$ $(\mathrm{BeV}/c)^2$ does not depend crucially on the detailed shape of the trajectory; in particular, we sug-

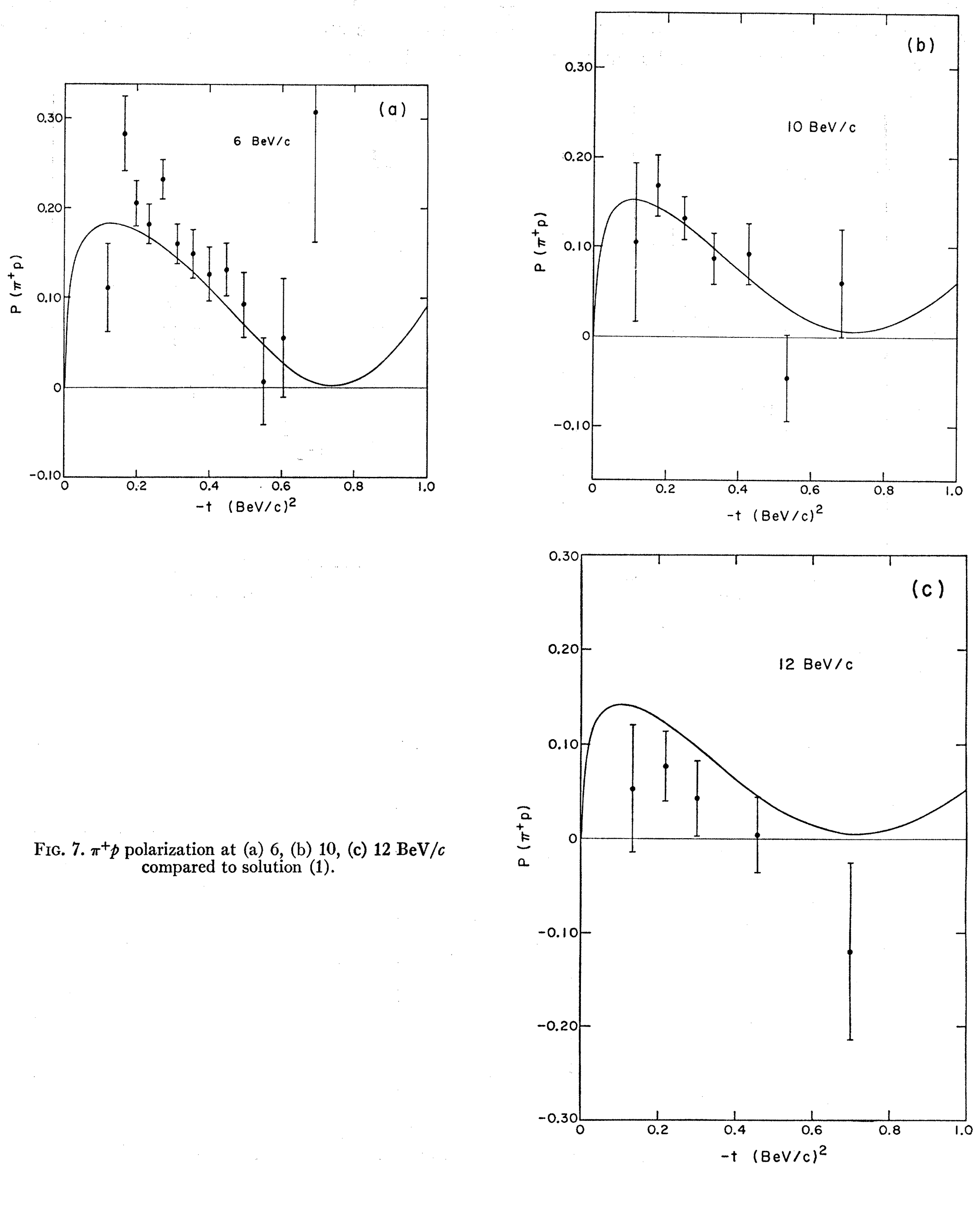

FIG. 7. π^+p polarization at (a) 6, (b) 10, (c) 12 BeV/c compared to solution (1).

gest, a trajectory such as the one indicated by the dotted line in the figure should also give an adequate fit to the NN data.

(iv) *Factorization tests.* Factorization severely constrains the analysis, and the fact that the solutions have been found is itself a test of compatibility with this property. However, since the constraints apply to ratios of spin-flip to non-flip couplings, the test would be made stronger if there were more polarization data.

In fact, we have found that a somewhat better χ^2 can be achieved if the factorization relationship between the πp and pp systems is released. On the other hand, we feel that the solutions which we have obtained incorporating factorization are reasonable and no incompatibility with it is seen in the results. We have not released the factorization constraints involved in the Sharp-Wagner formalism for the N-N amplitudes alone. Our assumption that low-lying trajectories can be lumped into the effects of the three particles which we keep explicitly is not exactly true when factorization is taken into account. Thus only if the effects of these particles are very small can we expect factorization to be well satisfied.

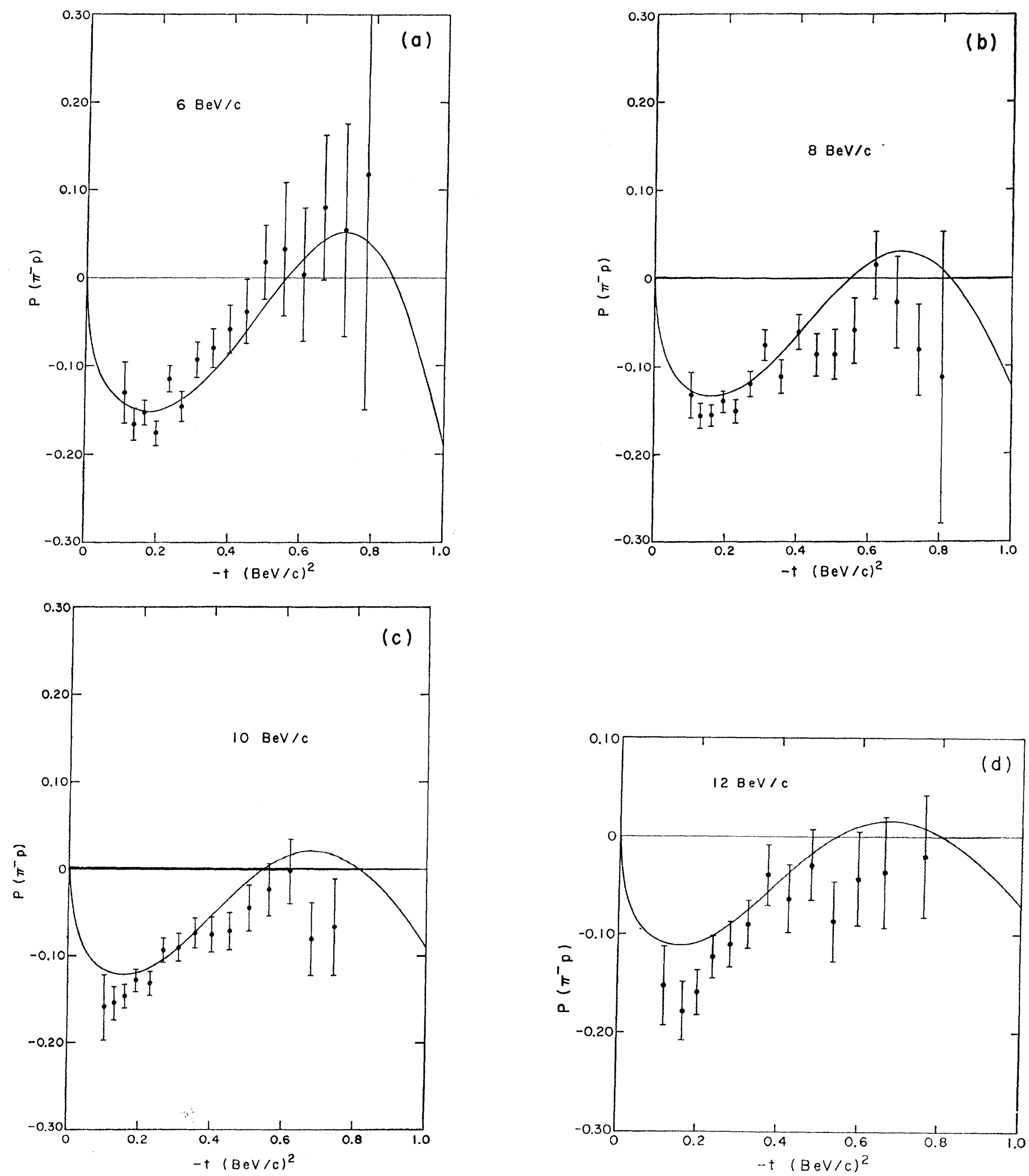

FIG. 8 π^-p polarization at (a) 6, (b) 8, (c) 10, and (d) 12 BeV/c compared to solution (1).

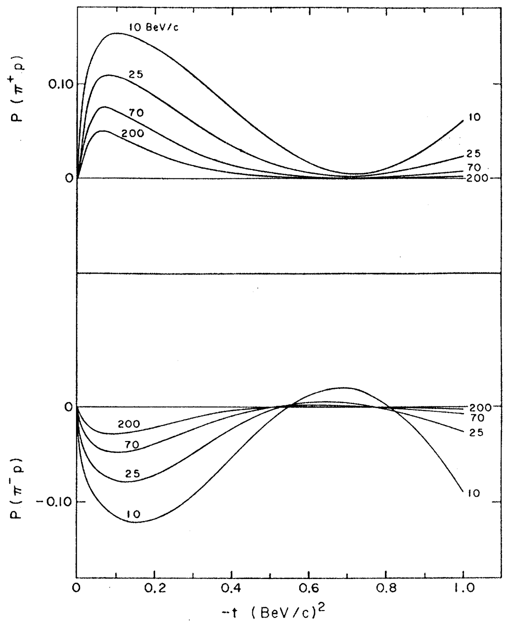

FIG. 9. Predictions from solution (1) for $\pi^{\pm}p$ polarizations at 10, 25, 70, and 200 BeV/c.

As an example of how factorization constrains the model, consider the polarized cross section $P(d\sigma/dt)$. All contributions are interference terms between pairs of Regge poles. In πN scattering, the P-P' interference terms can be separated at once, since they have the same sign for both π^+p and π^-p but the remaining terms change sign. Experimentally one finds that $\pi^{\pm}p$ polarizations are approximately mirror-symmetric, showing that

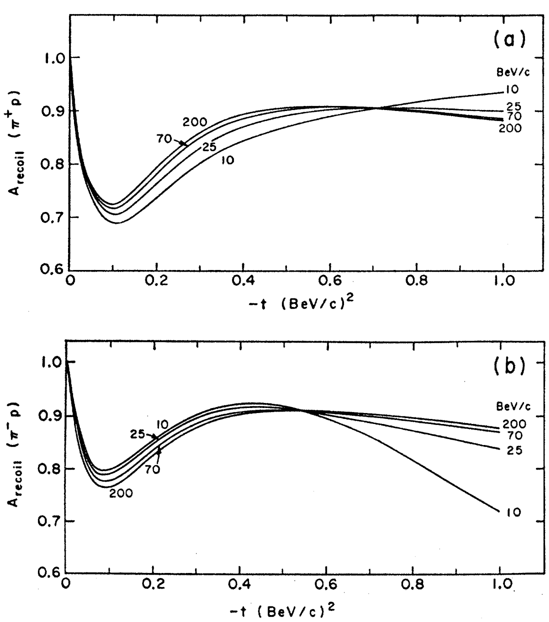

FIG. 10. A_{recoil} for (a) π^+p and (b) π^-p predicted by solution (2) for 10, 25, 70, and 200 BeV/c.

that the P-P' term is small. Factorization then predicts[34] that the P-P' term is also small for NN, and that the pp and $\bar{p}p$ polarized cross sections are roughly mirror-symmetric; (similarly for KN, approximate mirror symmetry is predicted for K^+p and K^-p). Measurements of polarization for $\bar{p}p$ (and also $K^{\pm}p$) will therefore provide rather transparent tests of factorization. The $\bar{p}p$ predictions are presented in Fig. 17.

It is interesting that the vanishing of P-P' interference in polarization, with the trajectories we use, also implies the vanishing of P-P' interference in the

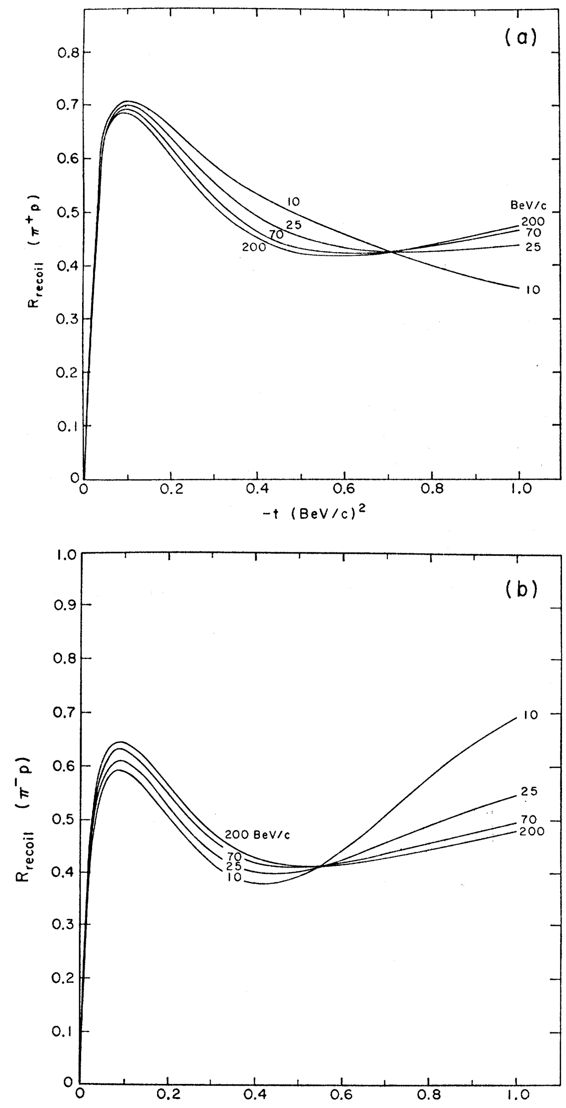

FIG. 11. R_{recoil} for (a) π^+p and (b) π^-p predicted by solution (1) for 10, 25, 70, and 200 BeV/c.

[34] In all cases, the $P-P'$ polarization term vanishes if both poles have the same phase, or both have the same ratio b_1/b_2. In our model, the first possibility does not happen. The second condition is enough to make the interference term in C_{NN} and K_{NN} vanish also (see Appendix C).

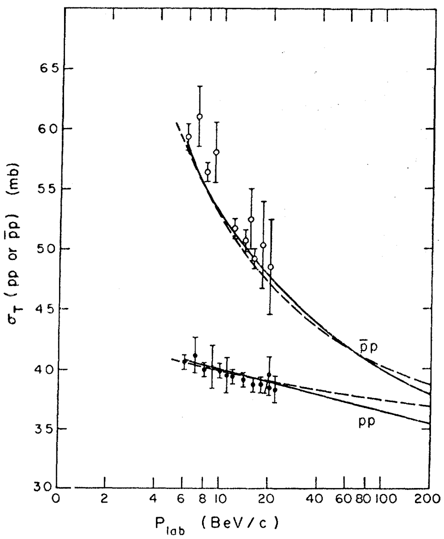

FIG. 12. Total cross sections from Ref. 17 for pp and $\bar{p}p$ compared to solution (1) with predictions up to 200 BeV/c (solid line) and also compared to solution (3) (dashed line).

second-rank spin tensors C_{NN} and K_{NN} (see Appendix C).[34]

The vanishing of the ω couplings at the crossover point (Sec. V.iii) offers further tests, since all ω contributions in other reactions must vanish at the same value of t. This is already checked for KN and $\bar{K}N$ scattering.[3,30] It is a severe constraint on the use of ω in explaining $K+N\rightarrow K^*+N$, for example.

(v) *Sum-rule constraints.* The sum rule associated with the $I=0$ Regge trajectories originally developed

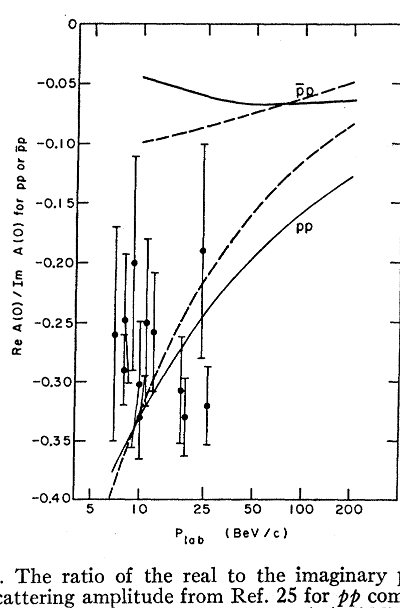

FIG. 13. The ratio of the real to the imaginary part of the forward scattering amplitude from Ref. 25 for pp compared with solution (1) with predictions up to 200 BeV/c (solid line) and also compared with solution (3) (dashed line). The forward scattering amplitude $A(0)$ is either ϕ_1 or $\phi_3(=\phi_1)$ and is given by Eq. (8). Predictions for $\bar{p}p$ are also given for solutions (1) and (3).

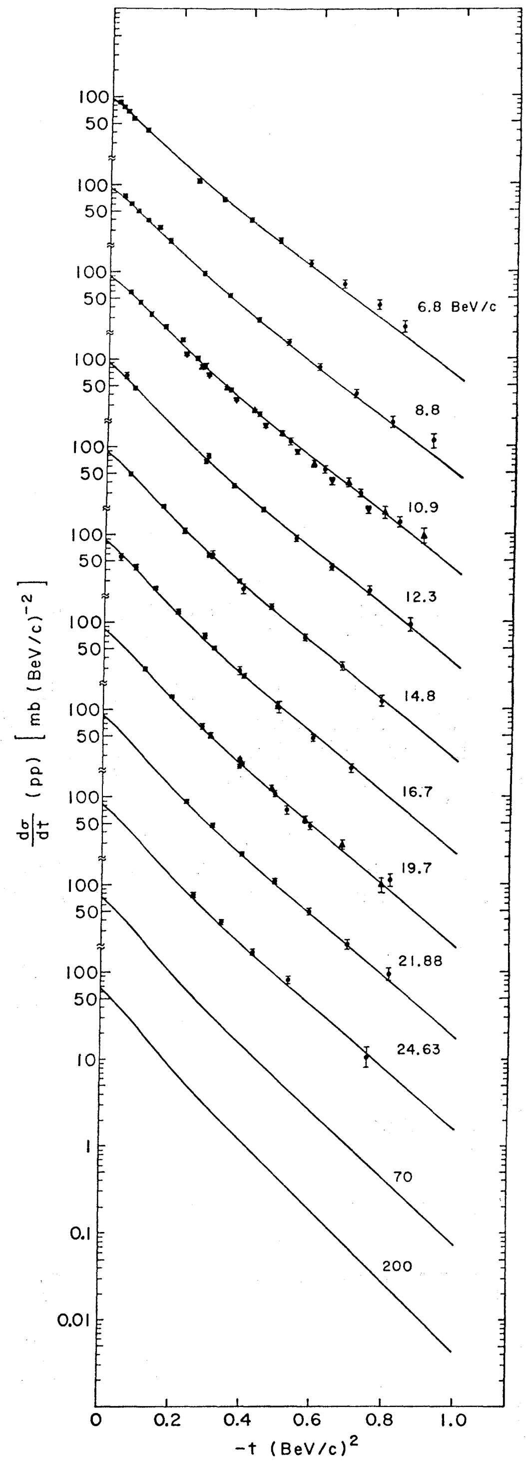

FIG. 14. pp differential cross sections at 6.8, 8.8, 10.9, 12.3, 14.8, 16.7, 19.7, 21.88, and 24.63 BeV/c compared to solution (1), with predictions up to 200 BeV/c. Successive sets of data are spaced by a decade.

by Igi[35] has recently been modified and the numerical analysis brought up to date by Scanio,[36] using data which have become available since Igi's analysis was made. A corresponding sum rule for $I=1$ trajectories[37] has been developed by Restignoli, Sertorio, and Toller, and recently also discussed by Igi and Matsuda. The question which we must answer here is the extent to which this sum rule should be used to restrict the allowed values for the parameters used in the χ^2 search, particularly the intercepts of the P' and ρ.

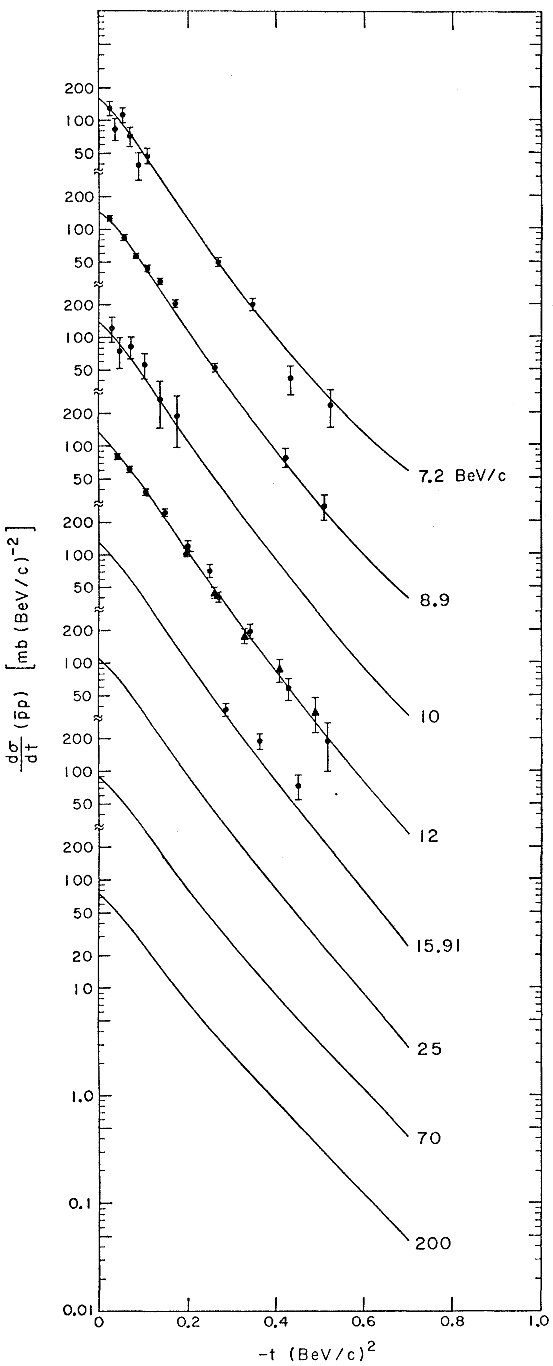

FIG. 15. $\bar{p}p$ differential cross sections at 7.2, 8.9, 10, 12, and 15.91 BeV/c compared to solution (1), with predictions up to 200 BeV/c. Successive sets of data are spaced by a decade.

For the $I=0$ forward scattering amplitude, we find from Eq. (8) of Ref. 36, after some trivial modifications,

$$2C_0{}^Px+(\alpha_{P'}+1)C_0{}^{P'}x^{\alpha_{P'}} = -2\pi^2(1+\mu/M)a_+ - \pi f^2/2M+\pi I(\mu)\,, \quad (27)$$

where

$$I(\mu)=\frac{1}{\pi}\int_\mu^x \frac{\omega' d\omega'}{(\omega'^2-\mu^2)^{1/2}}[\sigma_T(\pi^+p)+\sigma_T(\pi^-p)]\,, \quad (28)$$

and we use the relations between the C_i of Scanio and the $C_0{}^i$ of this paper: $C_P=2C_0{}^P$, $C_{P'}=\alpha_{P'}(\alpha_{P'}+1)C_0{}^{P'}$.

Using values for a_+ and $f^2/4\pi$ of -0.001 ± 0.003 (in natural units) and 0.081 ± 0.002, respectively,[38] we find that the first two terms on the right in Eq. (27) contribute 0.06 ± 0.19 mb BeV^2 and -0.66 ± 0.02 mb BeV^2, respectively. We use the value $\pi I(\mu)=195.4 \pm1.3$ mb BeV^2, as given by Scanio for $x=6$ BeV. Thus we find the contraint

$$H_0\equiv 2C_0{}^Px+(\alpha_{P'}+1)C_0{}^{P'}x^{\alpha_{P'}} =194.8\pm1.3 \text{ mb BeV}^2. \quad (29)$$

To obtain this equality it is clear that an explicit assumption has been made that P and P' are the only significant Regge poles beyond 6 BeV/c. To be specific, suppose that there is a low-lying Regge trajectory with intercept $\alpha_{P''}$. Then we would have a new H_0:

$$\overline{H_0}=2C_0{}^Px+(\alpha_{P'}+1)C_0{}^{P'}x^{\alpha_{P'}}+(\alpha_{P''}+1)C_0{}^{P''}x^{\alpha_{P''}} =x[\sigma_T{}^P+(\sigma_T{}^{P'}/\alpha_{P'})+(\sigma_T{}^{P''}/\alpha_{P''})]\,, \quad (30)$$

where $\sigma_T{}^i$ is the contribution of the i'th pole to the total cross section. If Eq. (29) is satisfied within one standard deviation, this would imply that at 6 BeV any further contribution to σ_T must satisfy

$$\sigma_T{}^{P''}\leqslant(1.3/194.8)(\sigma_T{}^P+\sigma_T{}^{P'}/\alpha^{P'})\,|\alpha_{P''}|\,.$$

For our solution (1), for instance, this implies

$$\sigma_T{}^{P''}<0.009\,|\alpha_{P''}|\,\sigma_T\,.$$

Since we have not taken other possible poles or a background integral into account, and in any case we do not feel that the Regge amplitudes are this accurately known at 6 BeV/c, we feel that this constraint is too stringent to be used directly in the χ^2 search. The sum rule is in fact included in the search, but the error used

[35] K. Igi, Phys. Rev. Letters **9**, 76 (1962).
[36] J. Scanio, Phys. Rev. **152**, 1337 (1966).
[37] M. Restignoli, L. Sertorio, and M. Toller, Phys. Rev. **150**, 1389 (1966); K. Igi and S. Matsuda, Phys. Rev. Letters **18**, 625 (1967).
[38] J. Hamilton, Phys. Letters **20**, 687 (1966); J. Hamilton and W. S. Woolcock, Rev. Mod. Phys. **35**, 737 (1963).

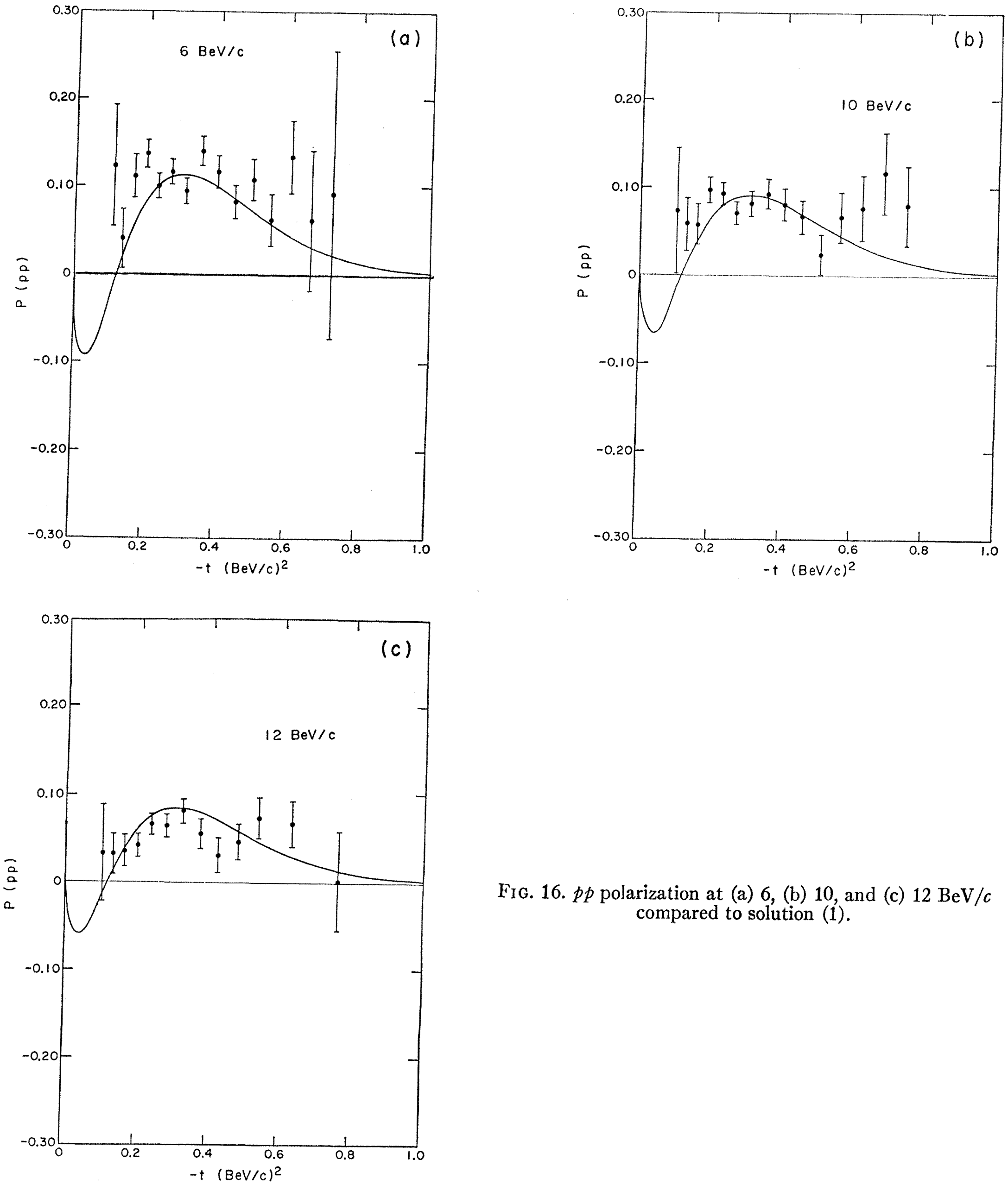

FIG. 16. pp polarization at (a) 6, (b) 10, and (c) 12 BeV/c compared to solution (1).

was increased from that in Eq. (29). The values of H_0 which we then obtain are

$$\begin{aligned} H_0 &= 192.0 \text{ mb BeV}^2, \quad \text{solution (1)}, \\ &= 193.5 \text{ mb BeV}^2, \quad \text{solution (1a)}, \\ &= 195.8 \text{ mb BeV}^2, \quad \text{solution (3)}. \end{aligned}$$

In view of the above discussion, we consider this to be reasonable agreement with Eq. (29).

For the $I=1$ amplitude, it can be shown that if the ρ is the only significant trajectory (ignoring lower-lying Regge poles and a background integral as before) one finds

$$\begin{aligned} H_1 &\equiv C_0{}^\rho x^{\alpha_\rho+1} \\ &= -\pi f^2 + \frac{1}{\pi}\int_\mu^x d\omega'(\omega'^2-\mu^2)^{1/2} \\ &\qquad \times[\sigma_T(\pi^-p)-\sigma_T(\pi^+p)]. \end{aligned} \tag{31}$$

The contribution to H_1 from the term in f^2 is -1.24 ± 0.03 mb BeV^2, whereas numerical evaluation of the

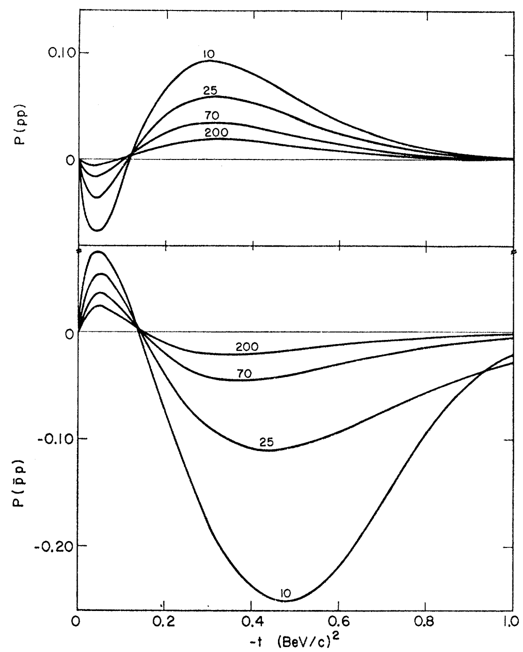

FIG. 17. Predictions from solution (1) for pp and $\bar{p}p$ polarizations at 10, 25, 70, and 200 BeV/c.

integral gives[39] 20.7±0.5 mb BeV^2, at $x=5$ BeV. Thus,

$$H_1=19.5\pm0.5 \text{ mb BeV}^2.$$

This constraint was also included in the search, but with a relaxation of the error. For our solutions we find

$$\begin{aligned} H_1&=18.7 \text{ mb BeV}^2, && \text{solution (1)},\\ &=19.1 \text{ mb BeV}^2, && \text{solution (1a)},\\ &=19.7 \text{ mb BeV}^2, && \text{solution (3)}. \end{aligned}$$

Again, agreement with the constraint seems reasonable.

(vi) *$\pi\pi$ predictions.* Up to now, there has been very little on which an estimate about $\pi\pi$ scattering at high energy could be made. Using equations given in Sec. II, factorization allows us to derive the P and P' terms in $\pi\pi$ scattering (i.e., the isospin-averaged[16] amplitude). This derivation assumes that our P' parameters are not greatly affected by contributions from A_2 or other poles not explicitly treated. Thus, from Eqs. (21)-(23) and (26) we are able to calculate the contributions to the total cross section and the differential cross section for $\pi\pi$ scattering. For solution (1) we find

$$\eta_\pi{}^P=1.90 \exp(0.27t)[\alpha_P(\alpha_P+1)]^{1/2}$$

and

$$\eta_\pi{}^{P'}=3.25 \exp(-0.62t)[\alpha_{P'}(\alpha_{P'}+1)]^{1/2},$$

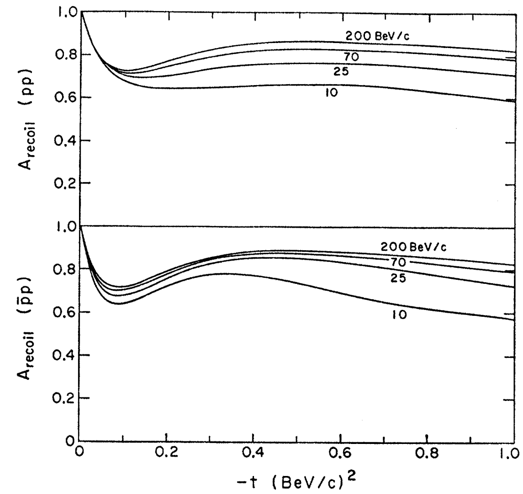

FIG. 18. A_{recoil} for pp and $\bar{p}p$ predicted by solution (1) for 10, 25, 70, and 200 BeV/c.

whereas for solution (3),

$$\eta_\pi{}^P=2.46 \exp(0.41t)\{\alpha_P(\alpha_P+1)(\alpha_P+2)/[\alpha_P(0)+2]\}^{1/2}$$

and

$$\eta_\pi{}^{P'}=2.83 \exp(-2.06t) \times\{\alpha_{P'}(\alpha_{P'}+1)(\alpha_{P'}+2)/[\alpha_{P'}(0)+2]\}^{1/2}.$$

Note that, although these expressions for $\eta_\pi{}^{P'}$ show an increasing exponential for increasing $|t|$, there is a strong decrease from the term in $\alpha_{P'}{}' \ln(s/s_0)$ so that for values of $s \gtrsim 5$ BeV^2, $A_{\pi\pi}$ has an over-all decrease with $|t|$.

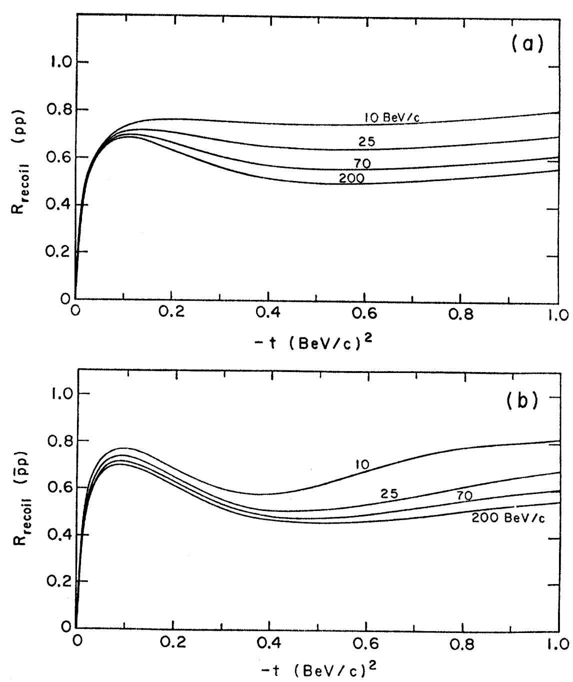

FIG. 19. R_{recoil} for (a) pp and (b) $\bar{p}p$ predicted by solution (1) for 10, 25, 70, and 200 BeV/c.

[39] We used the same set of data as that quoted in Ref. 36 for the numerical integration, except that for the $I=1$ case the integral is performed up to 5 BeV/c. The corresponding value obtained in the first of Ref. 37 is -19.8 ± 0.2 mb BeV^2. We feel that their error is slightly underestimated. To check our numerical calculation, we have recalculated H_0 with $x=6$ BeV. We found it to be 195.4±0.8 mb BeV^2, in perfect agreement with the results of Scanio.

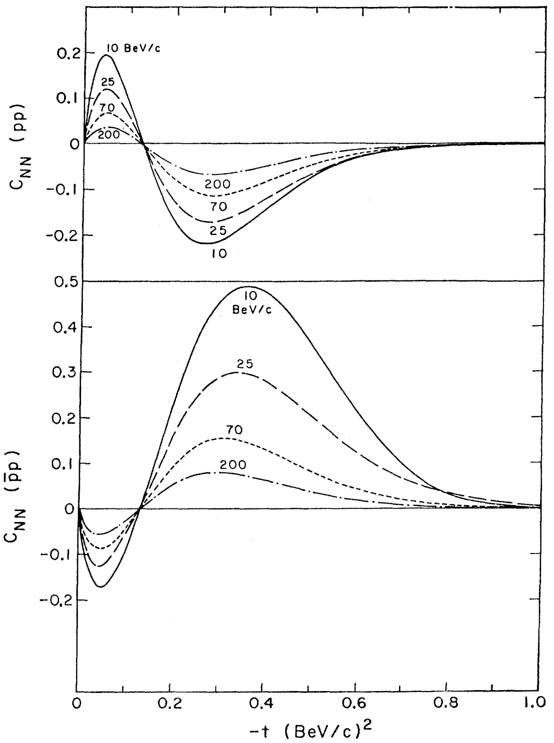

FIG. 20. C_{NN} for pp and $\bar{p}p$ scattering predicted by solution (1) for 10, 25, 70, and 200 BeV/c.

(vii) *Asymptotic limit.* Because the P' intercept is rather high, its contributions are not negligible until very high energies are reached. Thus for solution (1) the asymptotic NN, πN, and $\pi\pi$ total cross sections are 28.8, 14.5, and 7.3 mb, respectively, compared to 39.0, 47.7, 23.1, and 24.4 mb for pp, $\bar{p}p$, π^+p, and π^-p, respectively, at $s=40$ (BeV)^2 (corresponding to a laboratory momentum $\sim$20 BeV/c for the NN and πN cases). Using Eqs. (21), (23), and (26) we get a corresponding $\pi\pi$ total crosssection of 13.3 mb. The corresponding total cross sections at 70 BeV/c ($s=130$ BeV^2), corresponding to the future Serpukhov accelerator, are 37.0, 41.3, 20.7, 21.5, and 11.6 mb, respectively. For solution (3) we find corresponding asymptotic values of 34.8, 20.5, and 12.1 mb., whereas for $s=40$ (BeV)^2 the corresponding values are 39.1, 47.2, 23.8, 25.2, and 14.0 mb, and for $s=130$ (BeV)^2 they are 37.8, 41.4, 22.4, 23.2, and 13.2 mb. These values give an asymptotic ratio for NN to πN total cross sections of 1.99 for solution (1) and 1.70 for solution (3). This is to be compared with the predicted value of 1.5 which comes from the quark model.

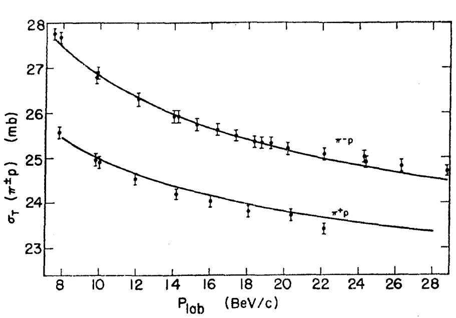

FIG. 21. Total cross sections from Ref. 26 for $\pi^{\pm}p$ compared with solution (3).

The continuing slow fall of total cross sections throughout the energy range of foreseeable accelerators is similar to that predicted by the model of Cabibbo *et al.*,[40] in which $\alpha_P(0)=0.93$ and the asymptotic limits are in fact zero.

(viii) *Dips and secondary maxima in π^-p charge-exchange, $\pi^{\pm}p$ elastic, and $\bar{p}p$ differential cross sections.* The dip in the charge-exchange differential cross section near $t=-0.6$ (BeV/c)^2 is explained here, as previously,[4,41] by the vanishing of B_ρ at $\alpha_\rho=0$. The secondary bump in the differential cross section is mainly contributed by the B_ρ amplitude. The dip and secondary bump structure has also been observed in both $\pi^{\pm}p$ and $\bar{p}p$ differential cross sections at lower energies, and in the case of $\pi^{\pm}p$ at higher momentum transfers. In our present analysis we have included only the data for higher energy (with P_L above 5.9 BeV/c) and small momentum transfer, $|t|<1$ (BeV/c)^2, but since this phenomenon is closely related to our work reported here, we would like to discuss this dip-bump phenomenon briefly. Recently it was pointed out by Mandelstam and Wang[42] that if the fixed-pole contribution in the J plane is dominant, then the dip phenomenon would be greatly suppressed. For the discussion which follows, we assume that the fixed-pole contribution is not important.

The dip-bump structure in both π^+p and π^-p differential cross sections as measured by the Michigan group[43] is quite pronounced in the 2.4–4-BeV/c region for the $|t|$ interval between 0.8 to 2.0 (BeV/c)^2. The

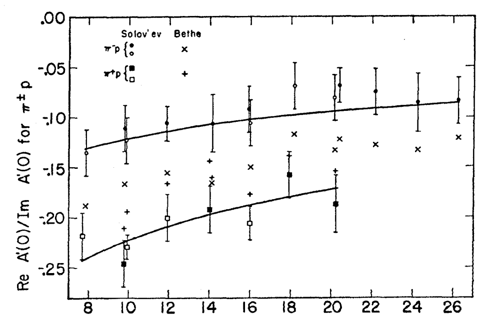

FIG. 22. The ratio of the real to the imaginary part of the forward scattering amplitude for $\pi^{\pm}p$ scattering from Ref. 26 compared to solution (3). The circles and squares are for the Solov'ev correction; and the crosses and plusses, for the Bethe correction.

[40] N. Cabibbo, L. Horwitz, J. Kokkedee, and Y. Ne'eman, Nuovo Cimento **45**, 275 (1966).

[41] G. Höhler, J. Baacke, H. Schlaile, and P. Sonderegger, Phys. Letters **20**, 79 (1966); F. Arbab and C. Chiu, Phys. Rev. **147**, 1045 (1966).

[42] S. Mandelstam and L. L. Wang, Phys. Rev. **160**, 1490 (1967).

[43] C. T. Coffin, N. Dikmen, L. Ettlinger, D. Meyer, A. Saulys, K. Terwilliger, and D. Williams, Phys. Rev. Letters **15**, 838 (1965); **17**, 458 (1966).

magnitudes of the bumps for both π^+p and π^-p are comparable and are significantly larger than the contribution of known direct-channel resonances nearby. The bumps fall off smoothly as the energy increases. These facts imply that the bumps are dominated by t-channel $I=0$ exchange. Frautschi suggested[7] that the main contribution to the bump could be associated with the P' trajectory. Analogously to the case of charge exchange, this contribution might come mainly from $B_{P'}$, and the minimum in t prior to the rise of the bump is then to be associated with the vanishing of $B_{P'}$ at $\alpha_{P'}=0$. He pointed out that this mechanism would be feasible if the P' coupling incorporates the Chew ghost-killing mechanism [see Eq. (2)]. On the other hand, it was suggested by Wang[8] that if the P' interacts in accordance with the no-compensation mechanism, both $A'_{P'}$ and $B_{P'}$ would vanish at $\alpha_{P'}=0$ [see Eqs. (1′) and (2′)]. Since these suggestions were made, the secondary bump data for both $\pi^{\pm}p$ and $\bar{p}p$ have been analyzed in some detail. As summarized in Ref. 9, it is found that the πp and $\bar{p}p$ dip-bump structure together with the high-energy πN and NN cross-section data can be satisfactorily explained with the no-compensation mechanism for the P' trajectory. With this mechanism the $\pi^{\pm}p$ secondary bump has been associated mainly with $A'_{P'}$. On the other hand, with Chew's ghost-killing mechanism for the P', the fits found were less satisfactory even for the πN data alone. In our present solution, we also find P' is preferred to be quite steep even though we have not included any low-energy data in the search [see also V.i]. However, our fits for solutions (1), (1a), and (2) are not too sensitive to the exact value of the slope. It could vary between 1 and 2 $(\text{BeV}/c)^{-2}$. We fixed it at 1.5. On the other hand, the fit for solution (3) actually preferred a larger slope.

For the NN differential cross section, the dip-bump structure occurs only in the $\bar{p}p$ differential cross section (observed unambiguously only *below* 2.5 BeV/c), and the pp differential cross section in the same region is rather smooth. Thus we feel that the $\bar{p}p$ dip-bump structure is generated by a rather delicate interference effect between the P and P' amplitudes and the ω amplitude in the low-energy region. (See Ref. 9 for a qualitative example of the fit with this interference effect.) Since we have not included these low-energy

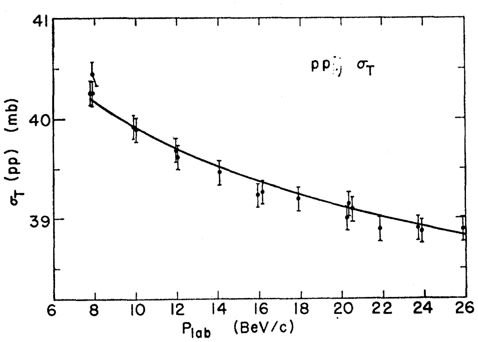

FIG. 23. Total cross sections from Ref. 26 for pp compared to solution (3).

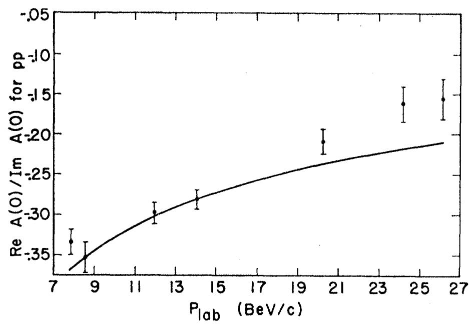

FIG. 24. The ratio of the real to the imaginary part of the forward scattering amplitude from Ref. 26 for pp compared with solution (3).

data in the present analysis and all the high-energy $\bar{p}p$ data included are smooth in the dip region, we did not anticipate that our solutions would produce this delicate low-energy effect.

(ix) *Polarization parameter P*. Because flip and nonflip terms have the same phase for a given Regge pole, polarization can come only from interference between different poles, with a resultant asymptotic s dependence: $P \sim s^{-|\alpha_1-\alpha_2|}$, where α_1 and α_2 are the two highest trajectories.

For πN scattering, the P-ρ and P'-ρ interference terms, with opposite signs for π^+p and π^-p elastic polarization, seem to dominate. The P-P' term has the same sign for both, and is found to be relatively small. Experiment seems to require the latter to be positive at 6 BeV/c and negative at 12 BeV/c [44]; this is of course impossible for the simple P-P' term in our model, but could come from interference with the exchange of a third $I=0$ pole.

Our model gives no polarization in $\pi^-+p\to\pi^0+n$, though some is observed.[22] It is not yet clear what new ingredient should be added; suggestions to date include another Regge pole[45] ρ', s-channel resonances,[46]

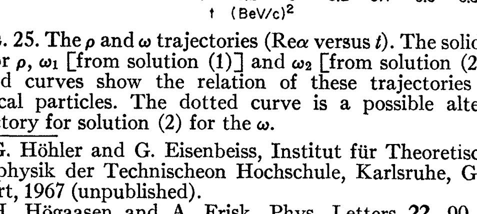

FIG. 25. The ρ and ω trajectories (Reα versus t). The solid curves are for ρ, ω_1 [from solution (1)] and ω_2 [from solution (2)]. The dashed curves show the relation of these trajectories to the physical particles. The dotted curve is a possible alternative trajectory for solution (2) for the ω.

[44] G. Höhler and G. Eisenbeiss, Institut für Theoretische und Kernphysik der Technischeon Hochschule, Karlsruhe, Germany Report, 1967 (unpublished).

[45] H. Högaasen and A. Frisk, Phys. Letters **22**, 90 (1966); H. Högaasen and W. Fischer, *ibid.* **22**, 516 (1966); R. K. Logan, J. Beaupre, and L. Sertorio, Phys. Rev. Letters **18**, 259 (1967); W. Rarita and B. Schwarzschild, Phys. Rev. **162**, 1378 (1967).

[46] R. J. N. Phillips, Nuovo Cimento **45**, 245 (1966); R. K. Logan and L. Sertorio, Phys. Rev. Letters **17**, 834 (1966); B. R. Desai, D. T. Gregorich, and R. Ramachandran, *ibid.* **18**, 565 (1967).

and Regge cuts.[47] The calculations incorporating these suggestions indicate that, whichever choice is made, no large corrections to the elastic or charge-exchange scattering occur.

For pp and $\bar{p}p$ polarization, the P-P' interference term must be small, from the πN result plus factorization [see (iv) above]. The P-ω and P'-ω terms have opposite signs for pp and $\bar{p}p$,and also have to vanish at the crossover point where all ω residues vanish [see (iii) above]. If the ω trajectory were to pass through zero, the P-ω and P'-ω interference terms would change sign. Note that the pp polarization shows no evidence of a sign change for $0.2 \leqslant |t| \leqslant 0.7$. Thus for our solutions (1), (1a), and (3), we find ω trajectories which have a relatively small slope.

(x) *Second-rank polarization tensors.* (See also Appendix C.) For πp scattering, in addition to P there is only the depolarization tensor D_{ij}, with two nontrivial elements D_{KK} and D_{KP}. To measure them one needs a polarized target, with recoil polarization analysis. As a practical point, note that target polarization *in the scattering plane* is needed. In practice, one probably measures linear combinations of these elements, in the form of Wolfenstein R_{recoil} and A_{recoil} parameters.

For pp and $\bar{p}p$ scattering, however, there are the depolarization, polarization-transfer, and spin-correlation tensors: D_{ij}, K_{ij}, and C_{ij}. Because our model contains no pseudoscalar or pseudovector trajectories, D_{ij} again has only two nontrivial elements D_{KK} and D_{KP}, while C_{ij} and K_{ij} have only one nonzero element between them: $C_{NN}=K_{NN}$. Because of factorization, for a single Regge pole we have

$$D_{ij}(\pi p)=D_{ij}(pp)=D_{ij}(\bar{p}p)\,,$$
$$C_{ij}(pp)=C_{ij}(\bar{p}p)=0\,.$$

Figures 10, 11, 18, and 19 show predictions for the depolarization tensor, in the form of the Wolfenstein parameters R_{recoil} and A_{recoil}, for 10, 25, 70, and 200 BeV/c. As expected, the $\pi^{\pm}p$, pp, and $\bar{p}p$ results become similar as the Regge pole P becomes dominant.

Figure 20 shows predictions for C_{NN} for pp and $\bar{p}p$ scattering at 10, 25, 70, and 200 BeV/c. Since C_{NN} depends on interference between different Regge poles, it decreases asymptotically just as does the polarization P:

$$C_{NN}\sim s^{-|\alpha_1-\alpha_2|}\,.$$

Factorization requires the P-P' interference to be small, since this interference is small[34] in $P(\pi N)$. The remaining P-ω and P'-ω interference terms are mirror-symmetric for pp and $\bar{p}p$, and vanish at the crossover point where ω residues vanish.

(xi) *Asymptotic spin dependence.* An important property of Regge poles is that they permit nontrivial spin dependence asymptotically. This contrasts with the diffraction picture, which suggests that summing

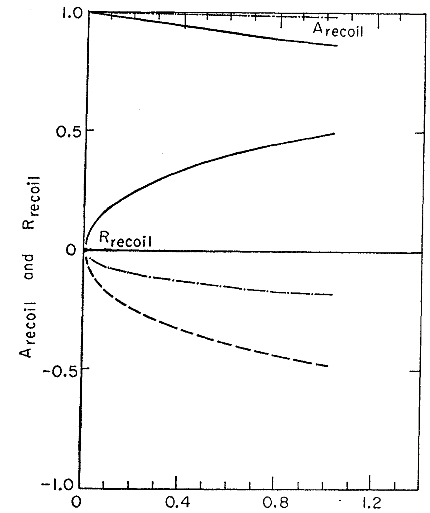

FIG. 26. A_{recoil} and R_{recoil} for some simple models at 20 BeV/c: (a) $B=0$ (solid line), (b) $H=0$ (dash-dot line), and (c) $f_{+-}=0$ (dashed line). For A_{recoil}, (a) and (c) effectively coincide.

over many inelastic intermediate states will leave no preferred spins.

On the other hand, it is not clear exactly what "no spin dependence" should mean, for the "natural" definition depends on the formalism used. Take πN scattering, for example: According to whether we describe the nucleon spin by a c.m. Dirac spinor, or a rest-frame Pauli spinor, or a c.m. helicity state, the "natural" definition of no spin dependence is $B=0$, or $H=0$, or $f_{+-}=0$ (where f_{+-} is the c.m. helicity-flip amplitude).[48] These are not equivalent.

To test for asymptotic spin dependence experimentally, we need the second-rank spin tensor D_{ij} (since we expect P and $C_{NN}\to 0$). Figure 26 shows predictions for the πp depolarization parameters R_{recoil} and A_{recoil} at 20 BeV/c, for comparison with the predictions of our model—and with eventual experiments—for the three definitions of "no spin dependence" given above.

(xii) *πN amplitudes at $t=m_\rho^2$.* Calculations of the $\pi\pi\to\bar{N}N$ amplitudes for the state $I=1$, $J=1$ have been made by Singh and Udgaonkar,[49] and by Ball and Wong,[50] in which the experimental information on the nuclear-charge and magnetic-moment form factors was used. From these results the amplitudes at the mass of the ρ ($t=m_\rho^2$) were obtained by Desai.[51] Comparing Eq. (4) of Ref. 51 and our Eqs. (1), (2), and (6) for the ρ amplitudes, we find

$$R_+=C_0{}^\rho[(1+C_2{}^\rho)\exp(C_1{}^\rho m_\rho{}^2)-C_2{}^\rho]$$
$$=\frac{2^{\alpha_\rho}\pi^{1/2}(2\alpha_\rho+1)\Gamma(\alpha_\rho+\frac{1}{2})8\pi M_N r_+}{\Gamma(\alpha_\rho+1)(4M_N{}^2-m_\rho{}^2)}$$
$$=13.7\text{ mb BeV}\,,$$

[47] V. M. de Lany, D. J. Gross, I. J. Muzinich, and V. L. Teplitz, Phys. Rev. Letters **18**, 149 (1967); C. B. Chiu and J. Finkelstein, Nuovo Cimento **48**, 821 (1967).

[48] M. Jacob and G. C. Wick, Ann. Phys. (N. Y.) **7**, 404 (1959).
[49] V. Singh and B. M. Udgaonkar, Phys. Rev. **128**, 1820 (1962).
[50] J. S. Ball and D. Y. Wong, Phys. Rev. **130**, 2112 (1963).
[51] B. R. Desai, Phys. Rev. **142**, 1255 (1966).

and

$$R_{-}=D_0{}^{\rho}\exp(D_1{}^{\rho}m_\rho{}^2)=\frac{2^{\alpha_\rho}\pi^{1/2}\Gamma(\alpha_\rho+\frac{1}{2})4\pi r_{-}}{\Gamma(\alpha_\rho+1)M_N{}^2}=34.8\text{ mb}.$$

To obtain these results one must identify Desai's amplitude A' with $\sqrt{2}$ times the A'_ρ used in this paper, and the approximations $s/2M_N{}^2\approx E/E_0$ and $4k^2\approx s$ must be used. The $r_\pm$ are defined by Desai and are found by him to be $r_+=0.87$ and $r_-=3.98$ (no errors were quoted for these numbers).

In our fit, we found that the data in the $t\geqslant 0$ region are not very sensitive to $R_\pm$, in particular to the value of R_+. Solution (1) is obtained without including $R_\pm$ in the fit, whereas solution (3) includes them. As mentioned in the results section, solution (1a) is obtained with the same conditions as (1) except that the $R_\pm$ constraints discussed here are imposed. The $R_\pm$ values for solutions (1), (1a), and (3) are as follows:

	R_+	R_-
Solution (1)	4.4	32.1
Solution (1a)	13.0	31.8
Solution (3)	10.9	31.0

Note, aside from the $R_\pm$ constraints, most of the parameters and the quality of the fits for solutions (1) and (1a) are similar. A comparison of the solutions (1) and (1a) as exhibited in Tables I–V shows that, although individual parameters change when the constraints are imposed, there is relatively little change except for $C_1{}^0$ and $C_2{}^0$, and either solution fits the data reasonably well.

ACKNOWLEDGMENTS

The authors are grateful for many interesting and helpful conversations with their colleagues at the Lawrence Radiation Laboratory and the University of California, particularly with Dr. Goeffrey Chew, Dr. Joseph Lepore, and Dr. Ling-Lie Wang. One of us (W.R.) would also like to thank Dr. Burton Moyer for encouragement and the hospitality of the Physics Department at Berkeley.

APPENDIX A: UNITARITY TEST OF THE DIFFRACTION EXPONENTIAL PEAK

We assume that the scattering amplitude $f(t)$ has the form $f(t)=iCe^{at}$. Our task is to obtain a criterion as to when and how unitarity may be violated.

The partial-wave expansion for $f(t)$ is easily obtained from a result of Gegenbauer[52]:

$$iCe^{at}=iCe^{-2k^2a}\left(\frac{\pi}{4k^2a}\right)^{1/2}\times\sum_{l=0}^{\infty}(2l+1)I_{l+1/2}(2k^2a)P_l(\cos\theta),\quad\text{(A1)}$$

where we use $t=-2k^2(1-\cos\theta)$.

If we write

$$f(t)=\frac{1}{k}\sum_{l=0}^{\infty}(2l+1)a_lP_l,$$

then unitarity demands that $|a_l-\frac{1}{2}i|\leqslant\frac{1}{2}$. From the properties of $I_{l+1/2}(x)$, namely that $I_{l+1/2}(x)\geqslant 0$ and $I_{l-1/2}(x)\geqslant I_{l+1/2}(x)$, we see that unitarity must be violated in the S state ($l=0$) if at all. From the requirement that $|a_0-\frac{1}{2}i|>\frac{1}{2}$ and that

$$I_{1/2}(z)=(2\pi z)^{-1/2}(e^z-e^{-z}),$$

we find

$$C[1-e^{-4k^2a}]>4ak$$

for violation of unitarity in the S state. As $4k^2a\gg 1$ in practice, we get the simple condition $C\gtrsim 4ka$. When we use the optical theorem $\sigma_T=4\pi\,\mathrm{Im}f(0)/k$, this condition becomes $\sigma_T\gtrsim 16\pi a$.

APPENDIX B: PARTIAL-WAVE PROJECTIONS AND UNITARITY TESTS

1. Pion-Nucleon Scattering

Following Singh,[5] the pion-nucleon partial-wave amplitudes are easily obtained. The invariant amplitude A is given by

$$A=A'-\frac{E_L+t/4M}{1-t/4M^2}B,\quad\text{(B1)}$$

and the scattering amplitudes f_1 and f_2 are defined in such a way that

$$f=f_1+(\boldsymbol{\sigma}\cdot\hat{k}_f)(\boldsymbol{\sigma}\cdot\hat{k}_i)f_2,\quad\text{(B2)}$$

where $\hat{k}_f$ and $\hat{k}_i$ are unit vectors in the direction of the final and the initial pion three-momenta, respectively, and

$$\frac{d\sigma}{d\Omega}=\sum_{\text{spins}}|(\text{final}|f|\text{initial})|^2.$$

Then one finds

$$f_1=\frac{E+M}{8\pi s^{1/2}}[A+B(s^{1/2}-M)]$$

and

$$f_2=\frac{-(E-M)}{8\pi s^{1/2}}[A-B(s^{1/2}+M)],\quad\text{(B3)}$$

where E is the c.m. energy of the nucleon. The partial-wave projection formula for f is given by

$$a_{l\pm}=\exp[i\delta_{l\pm}]\sin\delta_{l\pm}=\tfrac{1}{2}k\int_{-1}^{+1}[f_1P_l(x)+f_2P_{l\pm1}(x)]dx,\quad\text{(B4)}$$

where $l\pm$ stands for the state with orbital momentum l and total spin $J=l\pm\frac{1}{2}$. We note that the partial-wave

[52] G. N. Watson, *Theory of Bessel Functions* (The Macmillan Company, New York, 1948), Second ed., p. 369; also J. V. Lepore pointed out that this equation can be obtained easily from the well-known partial-wave expansion of a plane wave by analytic continuation.

amplitudes in Ref. 3 are defined to be larger than those in Eq. (B4) by a factor of 2; and, further, the former are tabulated there in units BeV^2 mb ($=2.568$).

Thus far we have suppressed isotopic spin indices. The crossing relations between the direct channel $I=\frac{1}{2}, \frac{3}{2}$ amplitudes and the t-channel Regge amplitudes are given by

$$\begin{aligned} A^{I=3/2} &= A^{\pi^+p} = A_P + A_{P'} - A_\rho\,, \\ A^{I=1/2} &= A^{\pi^-p} + \tfrac{1}{2}A^{\text{cex}} = A_P + A_{P'} + 2A_\rho\,, \end{aligned} \tag{B5}$$

where A^{cex} is the charge-exchange amplitude. Parallel relations can also be written for the B amplitudes.

From Eqs. (B4) and (B5) we can readily obtain the partial-wave amplitudes for our solutions by numerical integration. The results for solution (1) at 10 BeV are presented in Fig. 27. In order that the partial-wave amplitudes be compatible with unitarity, it is of course necessary that $|S_{l\pm}|\leqslant 1$, where $S_{l\pm}=\exp(2i\delta_{l\pm})$. We find as illustrated in Fig. 28 for $I=\frac{3}{2}$, that if unitarity is violated, the value of l is quite large, and the partial-wave amplitude is quite small, but the imaginary part of a_{l-} is negative (as is seen in Fig. 27), which is forbidden by unitarity. A similar result is obtained for $I=\frac{1}{2}$. Further, as E_L is increased the violation of unitarity occurs only for larger l values. We feel that the violation occurs because of a small error in the form chosen for the parametrization of the amplitudes near the forward direction, since the contribution to the high l partial waves comes predominantly from this region. This difficulty with unitarity is of the same kind as that found in Ref. 3.

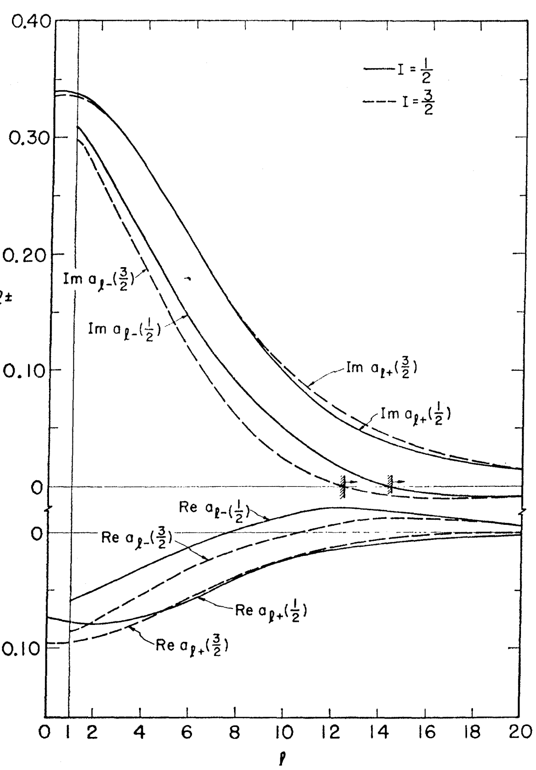

FIG. 27. Partial-wave amplitudes for πp scattering at 10 BeV. Real and imaginary parts of $a_{l\pm}$ for $I=\frac{3}{2}$ and $\frac{1}{2}$ based on solution (1).

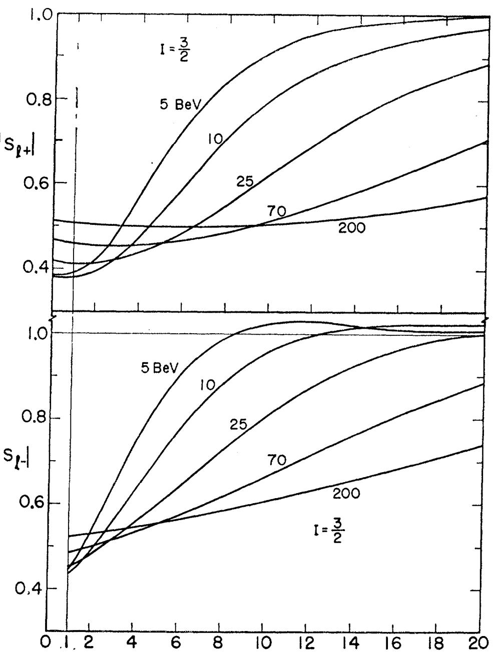

FIG. 28. Unitarity test for π^+p scattering. $|S_{l\pm}|$ for various energies based on solution (1).

2. Nucleon-Nucleon Scattering

In the case of nucleon-nucleon scattering, Goldberger *et al.*[53] chose partial-wave helicity amplitudes in the form

$$(\lambda_1'\lambda_2'|\phi|\lambda_1\lambda_2) = \frac{1}{p}\sum_J (2J+1)(\lambda_1'\lambda_2'|T^J(\omega)|\lambda_1\lambda_2)d_{\lambda\lambda'}{}^J(\theta)\,, \tag{B6}$$

where the λ_i, λ_i' are the helicities of particle i in the initial and final states, respectively, p is the momentum of either nucleon in the c.m. system, ω is the total c.m. energy, $d_{\lambda\lambda'}{}^J(\theta)$ is the reduced rotation matrix, and $\lambda=\lambda_1-\lambda_2$, and $\lambda'=\lambda_1'-\lambda_2'$. The partial-wave helicity matrices can be shown to be related to the partial-wave S matrices by

$$S^J = 1 + 2iT^J\,, \tag{B7}$$

where S^J is a unitary matrix in the space of the helicity components and **1** is a unit matrix in that space.[54] A

[53] M. L. Goldberger, M. J. Grisaru, S. W. MacDowell, and D. Y. Wong, Phys. Rev. **120**, 2250 (1960).

[54] The expression of Goldberger *et al.* (Ref. 53) differs from that of Jacob and Wick (Ref. 48) by a factor of 2, since the latter authors chose $T^J=-i(S^J-1)$. Note that both choices differ from that in Goldberger and Watson, [*Collision Theory* (John Wiley & Sons, Inc., New York, 1964)], in which $S^J=1-2\pi i\rho T^J$, where $\rho=p^2dp/dW$. In all cases, the S^J is the same—only the definition of T^J differs.

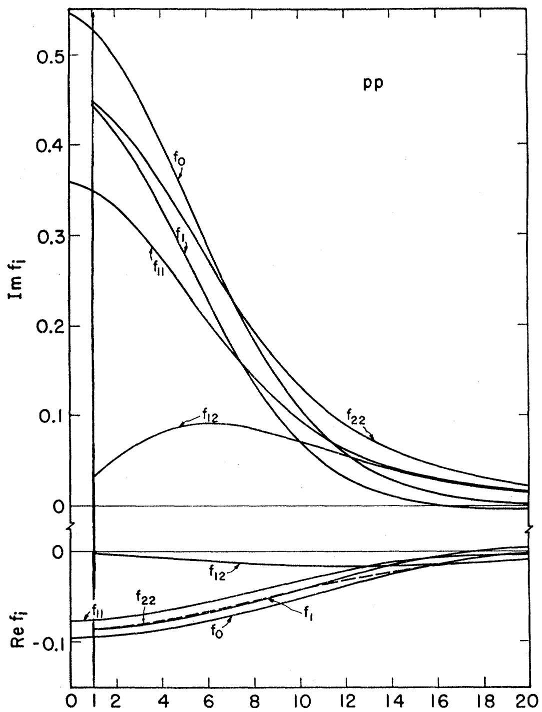

FIG. 29. Partial-wave amplitudes for pp scattering at 10 BeV. Real and imaginary parts of f_0, f_1, f_{11}, f_{12}, and f_{22} for pp given by solution (1). The dashed curve gives Ref_{22}.

unitary transformation corresponding to the selection of states of definite parity reduces S^J to its irreducible parts. This transformation leads to $f_0{}^J$ (the singlet amplitude), $f_1{}^J$ (the $J=l$ triplet amplitude), and $f_{11}{}^J$, $f_{12}{}^J$, and $f_{22}{}^J$ (the $J=l\pm1$ triplet amplitudes). For further details, see Ref. 53. These parts can be obtained using Eqs. (4.22), (4.23), and (4.25) of Ref. 53, which can be used for the partial-wave decomposition. [There is a misprint in Eqs. (4.25d) and (4.25e) of Ref. 53. The factor $1/(2J+1)$ outside the integrals should not be present.] The results of this analysis for solution (1) and $E_L=10$ BeV are presented in Figs. 29 and 30.

With the elements of S^J determined, one can immediately test those parts of S^J which correspond to the singlet and triplet states in which $J=l$ for compatibility with unitarity, i.e., $|S^J|\leqslant 1$. The parts corresponding to $J=l\pm1$ are slightly more complicated, since they are represented by a 2×2 matrix. In order that these be compatibile with unitarity, it is necessary that no more particles appear in all the final elastic-scattered channels of any spin state than were present initially and further that this be true for any linear combination of the initial spin states. If the initial state is represented by

$$\psi_{\rm in}=\begin{pmatrix} a \\ b \end{pmatrix},$$

where

$$|a|^2+|b|^2=1, \tag{B8}$$

the total number of particles going out in the elastic channels is

$$\begin{aligned} N_{\rm out}&=\sum |S^J\psi_{\rm in}|^2 \\ &=\psi_{\rm in}{}^\dagger S^{J\dagger}S^J\psi_{\rm in}, \end{aligned} \tag{B9}$$

where the sum is carried over all final spin helicities. If we write the 2×2 part of S^J as

$$S^J=\begin{pmatrix} S_{11} & S_{12} \\ S_{12} & S_{22} \end{pmatrix}, \tag{B10}$$

then

$$S^{J\dagger}S^J=\begin{pmatrix} |S_{11}|^2+|S_{12}|^2 & S_{11}S_{12}{}^*+S_{12}S_{22}{}^* \\ S_{11}{}^*S_{12}+S_{12}{}^*S_{22} & |S_{12}|^2+|S_{22}|^2 \end{pmatrix}. \tag{B11}$$

Finally, if $N_{\rm out}$ is varied with respect to a, b, subject to the constraint (B8), one finds that

$$\begin{aligned} |\bar{S}_{J=l+1}{}^1|^2\equiv N_{\rm out}{}^{\rm max}=\tfrac{1}{2}\{&|S_{11}|^2+|S_{22}|^2+2|S_{12}|^2 \\ &+[(|S_{11}|^2-|S_{22}|^2)^2+4|S_{11}S_{12}{}^* \\ &+S_{12}S_{22}{}^*|^2]^{1/2}\}. \end{aligned} \tag{B12}$$

This quantity was compared to one in testing unitarity. The results for the unitarity test are given in Fig. 31. As in the πp case, incompatibility again occurs only for large J, small f's, and Im$f<0$.

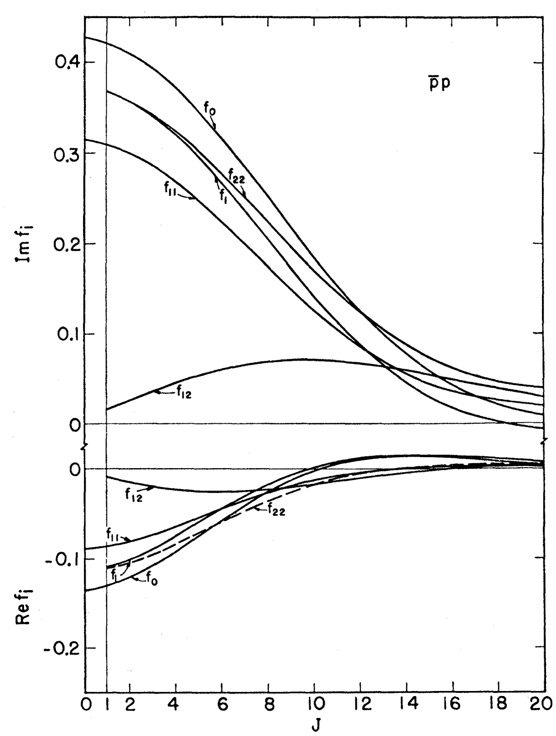

FIG. 30. Partial-wave amplitudes for $\bar{p}p$ scattering at 10 BeV. Real and imaginary parts of f_0,f_1,f_{11},f_{12}, and f_{22} for $\bar{p}p$ given by solution (1).

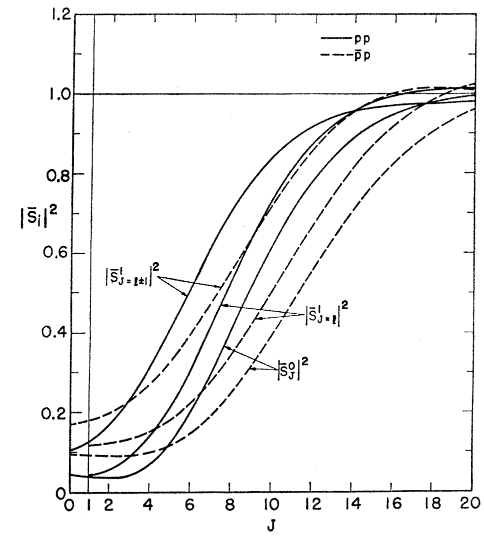

FIG. 31. Unitarity test. $|\bar{S}_J{}^0|^2$, $|\bar{S}_{J=l}{}^1|^2$ and $|\bar{S}_{J=l\pm1}{}^1|^2$ for pp (solid line) and $\bar{p}p$ (dashed line). For $J=l$, $\bar{S}_J\equiv S_J$, and for $J=l\pm1$, see Eq. (B12).

The partial-wave amplitudes are obtained by integrating the elastic amplitude over all angles from 0° to 180°, whereas the experimental data were restricted to the range $-t\lesssim 1$ (BeV/c)^2. Thus if the incident energy is 10 BeV, $\theta\lesssim 30°$. Hence a large part of the integration range lies in a region to which the scattering amplitudes must be extrapolated. A troublesome point is that the forms which were assumed have poles for large $|t|$, as the linear form assumed for $\alpha(t)$ goes through negative integers. Nevertheless, as a numerical matter this problem seems unimportant in determining the partial-wave amplitudes, since we removed the poles in various ways with no significant effect on those amplitudes. In one trial case the α's were bounded by a constant so that if the computed value of α were smaller, the bound was used, and in a second case the poles were removed by use of a product function like a gamma function. The small dependence (a few percent at most) on these changes is explained by the fact that for large $-t$ the amplitudes decrease rapidly and thus any residues at poles are very small.

APPENDIX C: POLARIZATION TENSORS

The discussion of polarization[55] is simpler if we describe nucleon spin states by Pauli spinors in the rest frame. This procedure is fully relativistic, but we must take account of certain rotations of spin axes between successive scatterings, in double- and triple-scattering experiments.[56]

The πN and NN c.m. scattering amplitudes have general forms

$$M_{\pi N}=G+iH\boldsymbol{\sigma}\cdot\mathbf{N}, \tag{C1}$$

$$M_{NN}=a+ic(\boldsymbol{\sigma}^{(1)}+\boldsymbol{\sigma}^{(2)})\cdot\mathbf{N}+m\boldsymbol{\sigma}^{(1)}\cdot\mathbf{N}\boldsymbol{\sigma}^{(2)}\cdot\mathbf{N}$$
$$+(g+h)\boldsymbol{\sigma}^{(1)}\cdot\mathbf{P}\boldsymbol{\sigma}^{(2)}\cdot\mathbf{P}+(g-h)\boldsymbol{\sigma}^{(1)}\cdot\mathbf{K}\boldsymbol{\sigma}^{(2)}\cdot\mathbf{K}. \tag{C2}$$

Here $\boldsymbol{\sigma}$ is the Pauli spin operator; $\mathbf{N}$, $\mathbf{P}$, and $\mathbf{K}$ are unit vectors along $\mathbf{k}_i\times\mathbf{k}_f$, $\mathbf{k}_f+\mathbf{k}_i$, and $\mathbf{k}_f-\mathbf{k}_i$; $\mathbf{k}_i$ and $\mathbf{k}_f$ are initial and final c.m. momenta; G, H, a, c, m, g, and h are scalar amplitudes, functions of s, t, and isospin; their connection to the πN amplitudes A' and B, and the NN helicity amplitudes ϕ_i, may be found in the literature.[5,57]

With Regge poles of the types we are considering (i.e., for 0^+, 1^-, 2^+, $\cdots$, etc., t-channel mesons), there are two simplifications. First, the coefficients g and h in Eq. (C2) vanish asymptotically compared to the others.[58] Henceforth we assume $g=h=0$ and use $\mathbf{N}$, $\mathbf{P}$, and $\mathbf{K}$ as convenient axes of reference. Second, the contributions of each pole to πN and NN amplitudes are simply related by factorization, asymptotically:

$$M(\pi N)=\sum_j \pm\frac{(s)^{1/2}}{8\pi}\xi_j\left(\frac{s}{s_0}\right)^{\alpha_j-1}\eta_{\pi j}(\eta_{Nj}+i\phi_{Nj}\boldsymbol{\sigma}\cdot\mathbf{N}), \tag{C3}$$

$$M(NN)=\sum_j \pm\frac{(s)^{1/2}}{8\pi}\xi_j\left(\frac{s}{s_0}\right)^{\alpha_j-1}(\eta_{Nj}+i\phi_{Nj}\boldsymbol{\sigma}^{(1)}\cdot\mathbf{N})$$
$$\times(\eta_{Nj}+i\phi_{Nj}\boldsymbol{\sigma}^{(2)}\cdot\mathbf{N}), \tag{C4}$$

where η_N and ϕ_N are defined in Sec. III, and j labels the Regge poles; the choice of the $+$ or $-$ sign depends on the signature of the pole and the particular process considered. Regge poles with odd G parity have $\eta_\pi=0$. $M(\bar{N}N)$ is the same as $M(NN)$ except for the sign of odd-signature terms. Note that Eq. (C4) gives a relation $c_j{}^2=-a_jm_j$ for each pole term; when one pole dominates, this applies to the whole amplitude.

Suppose the polarization of an initial state is described by a density matrix ρ_i in spin space. After scattering, the final density matrix is $\rho_f=M\rho_iM^\dagger$, where $M^\dagger$ is the Hermitian conjugate matrix to M, and the expectation value of any spin operator ξ_f is $\langle\xi_f\rangle=\mathrm{trace}(\rho_f\xi_f)/\mathrm{trace}(\rho_f)$. Thus polarization effects measure quantities of the form trace $(M\rho_iM^\dagger\xi_f)$.

The simpler possibilities for experimental measurements are these:

(a) No polarization initially, none measured finally; $\rho_i=1$, $\xi_f=1$. We get the unpolarized differential cross section $I_0=\mathrm{trace}(\rho_f)/\mathrm{trace}(\rho_i)$:

$$I_0(\pi N)=|G|^2+|H|^2, \tag{C5}$$

$$I_0(NN)=|a|^2+2|c|^2+|m|^2. \tag{C6}$$

[55] A somewhat fuller discussion is given in the reference in Ref. 14.
[56] H. P. Stapp, Phys. Rev. 103, 425 (1956).
[57] A. Scotti and D. Y. Wong, Phys. Rev. 138, B145 (1965).
[58] From Ref. 12 one can deduce that asymptotically $(g-h)\ll(g+h)$ and $(g+h)$ is order s^{-1} compared to a, c, and m.

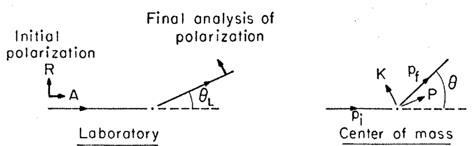

FIG. 32. Geometry for measurement of depolarization parameters, R and A, using a polarized incident beam.

(b) *One* polarization used either initially or finally: e.g., $\rho_i=1$, $\xi_f=\sigma_N^{(1)}$. We then get the polarization parameter P:

$$I_0P=\mathrm{trace}[MM^\dagger\sigma_N^{(1)}]=2\,\mathrm{Im}[GH^*]\quad\text{for }\pi N\qquad(\text{C7})$$

$$=2\,\mathrm{Im}[(a+m)c^*]\quad\text{for }NN.\qquad(\text{C8})$$

When a single pole dominates, all scalar amplitudes have the same phase and P vanishes.

(c) Particle 1 with initial polarization $\mathcal{P}$ in the j direction, final polarization of particle 1 analyzed in the k direction: $\rho_i=1+\mathcal{P}\sigma_j^{(1)}$, $\xi_f=\sigma_k^{(1)}$. The new term we get this way is an element of the depolarization tensor D_{jk}:

$$I_0D_{jk}=\mathrm{trace}(M\sigma_j^{(1)}M^\dagger\sigma_k^{(1)}).\qquad(\text{C9})$$

Referred to axes $\mathbf{N}$, $\mathbf{P}$, and $\mathbf{K}$, the off-diagonal elements of D constitute an antisymmetric tensor. Parity conservation makes $D_{KN}=D_{PN}=0$, in general, and $D_{NN}=1$ for πN scattering. The vanishing of g and h makes $D_{NN}=1$ for NN scattering also. There remain only two nontrivial elements:

$$I_0D_{KK}=I_0D_{PP}=|G|^2-|H|^2\quad\text{for }\pi N$$

$$=|a|^2-|m|^2\quad\text{for }NN,\qquad(\text{C10})$$

$$I_0D_{KP}=2\,\mathrm{Re}[GH]^*\quad\text{for }\pi N$$

$$=2\,\mathrm{Re}[(a-m)c^*]\quad\text{for }NN.\qquad(\text{C11})$$

When a single Regge pole dominates, Eqs. (C3) and (C4) yield[59]

$$D_{jk}(\pi N)=D_{jk}(NN),\qquad(\text{C12})$$

and this equality extends trivially to $\bar{N}N$, KN, and KN scattering as well.

(d) Particle 1 with initial polarization $\mathcal{P}$ in the j direction, final polarization of particle 2 analyzed in the k direction: $\rho_1=1+\mathcal{P}\sigma_j^{(1)}$, $\xi_f=\sigma_k^{(2)}$. This gives an element of the polarization transfer tensor K_{jk} (for NN only, there being no counterpart for πN):

$$I_0K_{jk}=\mathrm{trace}[M\sigma_j^{(1)}M^\dagger\sigma_k^{(2)}].\qquad(\text{C13})$$

As for D_{jk}, the off-diagonal elements of K constitute an antisymmetric tensor, and $K_{KN}=K_{PN}=0$ from parity conservation. The vanishing of g and h gives $K_{KK}=K_{PP}=K_{KP}=0$, and just one nontrivial element remains:

$$I_0K_{NN}=2\,\mathrm{Re}[am^*]+2|c|^2.\qquad(\text{C14})$$

[59] This result was first noticed by V. N. Gribov and I. Ya. Pomeranchuk, Phys. Rev. Letters **8**, 412 (1962).

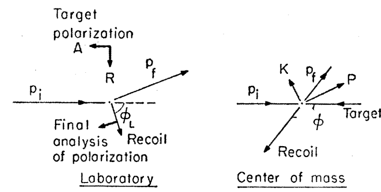

FIG. 33. Geometry for measurement of depolarization parameters, R and A, using a polarized target.

When one pole dominates, the factorization condition $c^2=-am$ makes even this element vanish.

(e) Both particles polarized initially (or analyzed finally): e.g., $\rho_i=1$, $\xi_f=\sigma_j^{(1)}\sigma_k^{(2)}$. This gives the spin correlation tensor C_{jk} (no counterpart for πN):

$$I_0C_{jk}=\mathrm{trace}[MM^\dagger\sigma_j^{(1)}\sigma_k^{(2)}].\qquad(\text{C15})$$

As for D_{jk}, C_{jk} is an antisymmetric tensor in its off-diagonal elements, and $C_{KN}=C_{PN}=0$ from parity conservation. The vanishing of g and h gives $C_{KK}=C_{PP}=C_{KP}=0$ and just one nontrivial element remains:

$$I_0C_{NN}=2\,\mathrm{Re}[am^*]+2|c|^2.\qquad(\text{C16})$$

This is exactly the same as K_{NN}, and vanishes for single-pole dominance.

(f) Higher-rank spin tensors can be defined,[60] but their measurement requires three or four polarization determinations. We shall not discuss them.

Thus the only nontrivial first- and second-rank polarization tensors with our model are P, $C_{NN}(=K_{NN})$, D_{KK}, and D_{KP}. The first two are usually measured directly; they involve polarizations normal to the scattering plane, and are unaffected by the spin-axis rotations.[56] Measurements of the depolarization tensor usually give linear combinations of D_{KK} and D_{KP}, and are affected by the spin-axis rotations.

The usual Wolfenstein[61] parameters R and A represent convenient experimental conditions. An incident beam has polarization $\mathcal{P}_i$ in the scattering plane; the scattered beam has transverse component of polarization $\mathcal{P}_f$, also in the scattering plane. According to whether the incident polarization is transverse or longitudinal, $\mathcal{P}_f=R\mathcal{P}_i$, or $\mathcal{P}_f=A\mathcal{P}_i$. The lab and c.m. geometries are shown in Fig. 32, where R and A are given by

$$R=D_{KK}\cos(\theta-\theta_L)-D_{KP}\sin(\theta-\theta_L),\qquad(\text{C17})$$

$$A=-D_{KK}\sin(\theta-\theta_L)-D_{KP}\cos(\theta-\theta_L),\qquad(\text{C18})$$

where θ and θ_L are c.m. and lab scattering angles.

With present-day techniques it is probably easier to use a polarized target instead of polarized incident beams, and analyzing the recoil polarization; indeed, for πN this is the only way to obtain information of D.

[60] L. Puzikov, R. Ryndin, and J. Smorodinsky, Nucl. Phys. **3**, 436 (1957); R. J. N. Phillips, Harwell Report No. AERE-R3141, 1960 (unpublished).
[61] L. Wolfenstein, Phys. Rev. **96**, 1654 (1954).

We define analogous measurements, denoting them R_{recoil} and A_{recoil}, in which the target has longitudinal (A_{recoil}) or transverse (R_{recoil}) polarization, and the recoil polarization is analyzed transversely. The geometries are shown in Fig. 33, The terms R_{recoil} and A_{recoil} are given by

$$R_{\text{recoil}}=D_{KK}\cos(\phi-\phi_L)+D_{KP}\sin(\phi-\phi_L)\,, \quad \text{(C19)}$$

$$A_{\text{recoil}}=D_{KK}\sin(\phi-\phi_L)-D_{KP}\cos(\phi-\phi_L)\,, \quad \text{(C20)}$$

where ϕ and ϕ_L are the c.m. and lab recoil angles, respectively.

APPENDIX D: REGGE SHRINKING

One of the earliest predictions for a single Regge pole is that differential cross sections "shrink" with increasing energy, because the trajectory has a positive slope in t. Experimentally, some cross sections shrink and some do not; this can be understood when several Regge poles take part. Here we illustrate this effect by deriving an "effective one-pole trajectory"; depending on the energy and the process considered, its slope may be positive or negative, giving shrinking or antishrinking.

A single Regge pole leads to cross sections of the general form

$$\frac{d\sigma}{dt}(E,t)=F(t)(E/E_0)^{2\alpha(t)-2}. \quad \text{(D1)}$$

If, given $d\sigma/dt$ in a many-pole situation, we choose to approximate it by the one-pole formula, the resulting effective one-pole trajectory is

$$\alpha_{\text{eff}}(E,t)=1+\frac{1}{2}\frac{d[\ln(d\sigma/dt)]}{d[\ln(E/E_0)]}\,, \quad \text{(D2)}$$

where α_{eff} varies with energy; its slope in t characterizes the degree of shrinking.

We now make a simplified model of πN scattering for small t by absorbing all the t dependence in exponential factors and neglecting spin-flip:

$$\frac{d\sigma}{dt}=|\sum_j A_j|^2E^{-2}\,, \quad \text{(D3)}$$

$$A_j=-C_j\exp[-i\phi_j+D_jt+\alpha_j\ln(E/E_0)]\,, \quad \text{(D4)}$$

where the Regge poles are labelled by $j(=P,P',\rho)$. The phase factor ϕ_j is $\frac{1}{2}\pi\alpha_j$ for P and P', but is $\frac{1}{2}\pi(\alpha_j+1)$ for ρ. Here C_j and D_j are numerical coefficients; C_ρ changes sign between π^+p and π^-p scattering. The trajectories are linear as before; $\alpha_j(t)=\alpha_j(0)+t\alpha_j'$. It is convenient to define $\tilde{D}=D_j+\alpha_j'\ln(E/E_0)$; these quantities determine the width of each pole contribution to the amplitude.

Assuming P is dominant, with $\alpha_P(0)=1$, and taking P' and ρ effects to first order, we obtain

$$\alpha'_{\text{eff}}(t=0)=1+(\sigma_{P'}/\sigma_P)[\alpha_{P'}(0)-1] +(\sigma_\rho/\sigma_P)[\alpha_\rho(0)-1]\,, \quad \text{(D5)}$$

$$\begin{aligned}\alpha'_{\text{eff}}(t=0)=\alpha'_P+(\sigma_{P'}/\sigma_P)\{[\alpha_{P'}(0)-1](\tilde{D}_{P'}-\tilde{D}_P)\\ +[\alpha'_{P'}-\alpha'_P]\{1-\tfrac{1}{2}\pi[1-\alpha_{P'}(0)]\\ \times\cot[\tfrac{1}{2}\pi\alpha_{P'}(0)]\}\}+(\sigma_\rho/\sigma_P)\{[\alpha_\rho(0)-1]\\ \times(\tilde{D}_\rho-\tilde{D}_P)+[\alpha'_\rho-\alpha'_P]\\ \times\{1+\tfrac{1}{2}\pi[1-\alpha_\rho(0)]\tan[\tfrac{1}{2}\pi\alpha_\rho(0)]\}\}\,, \quad \text{(D6)}\end{aligned}$$

where σ_P, $\sigma_{P'}$, and σ_ρ are the partial contributions to the total cross section for the particular process and energy being considered. With this definition, σ_ρ changes sign between π^+p and π^-p scattering. These relations show explicitly how $\alpha_{\text{eff}}\rightarrow\alpha_P$ as $\sigma_{P'}\rightarrow 0$ and $\sigma_\rho\rightarrow 0$, asymptotically.

The question of shrinking concerns the slope α'_{eff}. Equation (D6) shows that if the P' amplitude is more sharply peaked than that of P (i.e., $\tilde{D}_{P'}>\tilde{D}_P$), a positive contribution from α'_P can be offset, leaving $\alpha'_{\text{eff}}\approx 0$ and no net shrinking, in a range of energy. This is indeed what happens in the present paper and in previous analyses.[3,4] A second point to notice is the alternating sign of the ρ effect; if ρ increases the shrinking in π^+p scattering, it decreases the shrinking for π^-p scattering.

The argument above can be made also for pp and $\bar{p}p$ scattering (or for K^+p and K^-p), with ω taking the place of ρ. If ω tends to produce shrinking for pp (K^+p), it will tend to produce antishrinking for $\bar{p}p$ (K^-p): its contributions to α'_{eff} in the two cases will be equal and opposite. The argument can obviously be generalized to any number of secondary trajectories of the "normal-parity" type so far considered. Terms with odd signature change sign between pp and $\bar{p}p$; terms with isospin $I=1$ change sign between pp and pn; and so on.

TABLE VI. Values of α'_{eff} deduced from various experiments (see Ref. 62).

Reaction	α'_{eff} (BeV/c)$^{-2}$
$\pi^-p\rightarrow\pi^-p$	-0.062 ± 0.068
$\pi^+p\rightarrow\pi^+p$	0.103 ± 0.074
$\bar{p}p\rightarrow\bar{p}p$	-0.914 ± 0.376
$pp\rightarrow pp$	0.685 ± 0.051
$K^-p\rightarrow K^-p$	-0.398 ± 0.322
$K^+p\rightarrow K^+p$	$0.50\ \pm0.16$

Table VI, expressing results from Ref. 62, shows values of α'_{eff} deduced directly from experiment for various processes in the momentum range 6–25 BeV/c. These results suggest that most of the shrinking or antishrinking comes from the interference between P and the odd-signature poles ρ and ω.

[62] S. J. Lindenbaum, in *Proceedings of the Oxford International Conference on Elementary Particles, 1965* (Rutherford High-Energy Laboratory, Chilton, Berkshire, England, 1966).

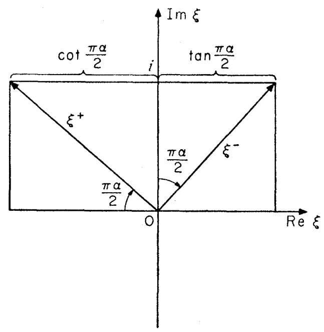

FIG. 34. Representations of $\xi^{\pm}$ in the complex plane.

APPENDIX E: APPLICATION OF VECTOR NOTATION TO THE SCATTERING PROBLEM

Instead of the usually employed complex algebra, we sometimes find it advantageous to use the mathematically equivalent vector notation, which has the virtue of compactness and of geometrical clarity.

To preserve mathematical equivalence, we require that: (i) the two components of a complex variable $A=A_1+iA_2$ go into the two components in a two-dimensional vector space $\mathbf{A}=(A_1,A_2)$, (ii) the operation $\mathrm{Re}(A^*B)=\mathrm{Re}(AB^*)=A_1B_1+A_2B_2\rightarrow\mathbf{A}\cdot\mathbf{B}$, and (iii) the operation $\mathrm{Im}(A^*B)=-\mathrm{Im}(AB)^*=A_1B_2-A_2B_1\rightarrow\mathbf{A}\times\mathbf{B}$.

We summarize some results on the signature factor ξ:

$$\xi^+=i-\cot\tfrac{1}{2}\pi\alpha=\frac{-\exp(-\frac{1}{2}i\pi\alpha)}{\sin\frac{1}{2}\pi\alpha},$$

$$\xi^-=i+\tan\tfrac{1}{2}\pi\alpha=\frac{i\exp(-\frac{1}{2}i\pi\alpha)}{\cos\frac{1}{2}\pi^{\alpha}}.$$

Note that: $\xi^-(\alpha)=\xi^+(\alpha\pm1)$. Also $|\xi^+|=1/\sin\frac{1}{2}\pi\alpha^+$ and $|\xi^-|=1/\cos\frac{1}{2}\pi\alpha^-$. In Fig. 34 we show the above relations in geometric form.

For πN scattering, let us define:

$$a=A'M_N(1-\tau)^{1/2}/(4\pi^{1/2}ks^{1/2})$$

and

$$b=\frac{B}{(\pi s)^{1/2}}\frac{M_N}{4k}\left(\frac{-\tau(4M_N{}^2p^2+st)}{4M_N{}^2(1-\tau)}\right)^{1/2},$$

where $\tau=t/4M_N{}^2$. Then Eqs. (6) and (7) take the simple forms

$$\frac{d\sigma}{dt}(s,t)=a^2+b^2, \qquad (6')$$

$$P(s,t)=\frac{-2[\mathbf{a}\times\mathbf{b}]}{a^2+b^2}. \qquad (7')$$

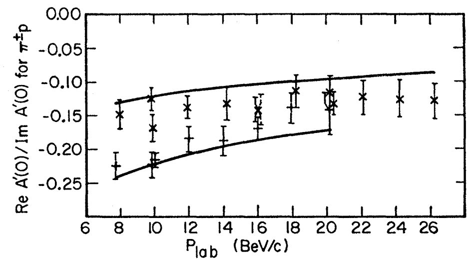

FIG. 35. The ratio of the real to the imaginary part of the forward scattering amplitude for π^+p scattering from Ref. 63 compared to solution (3). The upper curve (x) is for π^-p and the lower curve (+) is for π^+p.

We see immediately that if $|P|=1$ then $\mathbf{a}\perp\mathbf{b}$ and $a^2=b^2$. Also, if only two poles contribute to the scattering, then $\alpha^-=\alpha^+$ or $|\alpha_1{}^{\pm}-\alpha_2{}^{\pm}|=1$ for maximum polarization for fixed a and b.

To take full advantage of the vector notation, we introduce an additional vector space for the non-flip and flip factors, i.e.,

$$\mathfrak{B}_i=(1-\tau)^{1/2}(b_1{}^i,(-\tau)^{1/2}\alpha_ib_2{}^i)(E/E_0)^{(\alpha_i-1)/2}.$$

The formulas developed by Wagner[12] for NN scattering then become

$$\frac{d\sigma}{dt}=\frac{1}{16\pi}\sum_{i,j}\boldsymbol{\xi}_i\cdot\boldsymbol{\xi}_j(\mathfrak{B}_i\cdot\mathfrak{B}_j)^2,$$

$$P\frac{d\sigma}{dt}=\frac{1}{16\pi}\sum_{i,j}|\boldsymbol{\xi}_i\times\boldsymbol{\xi}_j|\,|\mathfrak{B}_i\times\mathfrak{B}_j|(\mathfrak{B}_i\cdot\mathfrak{B}_j).$$

As expected, the maximum polarization that can be attained from these formulas is 1. For example, when only two poles interfere, we require that $\boldsymbol{\xi}_1\perp\boldsymbol{\xi}_2$, $\xi_1{}^2=\xi_2{}^2$, $\mathfrak{P}_1{}^2=\mathfrak{P}_2{}^2$, and the angle in the $\mathfrak{B}$ space getween $\mathfrak{B}_1$ and $\mathfrak{B}_2$ is 45°. For instance, the first condition is satisfied if $\alpha_1(=\alpha^+)=0.5$ and $\alpha_2(=\alpha^-)=0.5$.

POSTSCRIPT

A month after this paper was received by the Physical Review revised data became available from Foley *et al.* on the phase of the forward amplitudes for $\pi^{\pm}p$ scattering.[63] In Fig. 35 we show these data together with the calculated values obtained from solution (3). Although the fit is not so remarkable as that shown in Fig. 22, we feel that it is good, especially in view of the estimated systematic error. A very similar result for the phase was obtained by Foley *et al.*[63] with the use of dispersion relations.

[63] K. J. Foley, R. S. Jones, S. J. Lindenbaum, W. A. Love, S. Ozaki, E. D. Platner, C. A. Quarles, and E. H. Willen, Phys. Rev. Letters **19**, 193 (1967).